Research Article

Geometric Morphometric Approaches to Acoustic Signal Analysis in Mammalian Biology

Norman MacLeod[a,*], Jonathan Krieger[b], Kate E. Jones[c]

[a]*Palaeontology Department, The Natural History Museum, Cromwell Road, London, SW7 5BD, UK*
[b]*Herbarium, Library, Art & Archives Directorate, Royal Botanic Gardens, Kew, Richmond, Surrey, TW9 3AB, UK*
[c]*Institute of Zoology, Zoological Society of London, Regents Park, London NW1 4RY, UK*

Abstract

In the quarter century since the development of geometric morphometrics the community of practitioners has largely been occupied with training issues and anatomy-based applications research in the biological sciences. However, just as the scope of geometry transcends comparative anatomy, the potential scope of morphometric analysis transcends investigations of the form and shape of organismal bodies. An important area of opportunity for morphometricians lies in the application of geometric methods to non-traditional form/shape analysis problems. To illustrate the potential of morphometric data analysis approaches to contribute to investigations outside its traditional base in (physical) morphology we report here results of an investigation into the morphometrics of bat echolocation calls. By treating Hanning windowed spectrograms of bat search echolocation calls as complex 3D surfaces, and by using a variant of eigensurface analysis to sample and compare these surfaces, it is possible to identify bat species to very high levels of accuracy (> 90% for raw cross-validated training set identifications, > 80% for jackknifed training set identifications), even for species (e.g., *Myotis*) whose spectrograms have resisted separation into species-specific clusters using traditional spectrogram descriptors. Moreover, the shape modeling capabilities of geometric morphometrics render the complex mathematical subspaces within which these spectrogram shape data reside – along with the discriminant functions used to separate training-set clusters – interpretable in a simple, intuitive, and biologically informative manner. These results demonstrate the rich source of species-specific information bioacoustic signal structures represent. They also illustrate the type of advances that can be made when morphometricians venture beyond the traditional confines of their field to address wider questions of significance in the biological and the physical sciences.

Introduction

It is commonplace to read that a revolution has taken place in morphometrics. When making such statements most authors refer to the development of what has come to be called "geometric morphometrics" (GM), a term that usually goes undefined even in review articles about it (e.g., Adams et al. 2004). A systematic evaluation of the morphometric literature reveals the presence of at least two competing definitions of GM. The larger proportion of articles, either explicitly or implicitly, identify it with a specific set of data-analysis procedures (e.g., Procrustes superposition, relative warps analysis, principal warps analysis) that were formulated originally to operate on Cartesian coordinate data directly, as multivariable data sets, without transforming them first into scalar distances angles, areas, form factors, etc. as was commonly the case prior to the 1990s. In our view this is the "weak" definition of GM; inadequate insofar as the technique lists offered are always exemplary rather than definitive and deficient in that no attempt is made to explain what unites these (and other) data analysis approaches together either mathematically or conceptually. This definition leads to confusing ambiguities and inconsistencies over what is, and what is not, a GM method.

The alternative "strong" definition of GM understands this to include only those aspects of shape analysis that are undertaken in a Kendall (or a mathematically similar) shape space (Kendall, 1984; Bookstein, 1991) or some lower dimensional derivative thereof. This is a set of hypothetical mathematical spaces – actually the surfaces of mathematical manifolds – unified by the fact that each point in the space corresponds to a possible configuration of n landmark or semilandmark points, usually after the canonical "nuisance" factors of position, size and rotation of have been eliminated from consideration. There are an infinite number of such shape spaces. These geometric spaces make no assumptions regarding the size of the landmark/semilandmark sets that fall into their domain (n can be any integer), the rules used to specify locations of the landmarks/semilandmarks, the nature of the objects on which these landmarks/semilandmarks are located, or the range of procedures used to analyze such shape coordinate data.

While this "strong" definition of GM has the advantage of enforcing conceptual consistency, it is perhaps too restrictive if it is understood to apply only to the subset of GM methods that operate in the Kendall shape space *sensu stricto* (e.g., principal warps analysis, relative warps analysis). For example, the outline data analysis methods of elliptical Fourier analysis (Kuhl and Giardina, 1982; Ferson et al., 1985) and eigenshape analysis (Lohmann, 1983; MacLeod, 1999) are employed routinely by geometric morphometricians, but neither operates in the Kendall shape space (see Bookstein 1991). However, if the concept of GM is extended to apply to all methods used to analyse data in which point in the space corresponds to a possible configuration of n landmark points however determined, elliptical Fourier analysis, eigenshape analysis, and a host of other data formulations can be used by GM practitioners to test form and shape-based hypotheses rigorously.

The conceptual synthesis responsible for geometric morphometrics can accommodate this ecumenical approach to shape space definition easily and, indeed, can reap substantial benefits from its employment. This synthesis took place some time ago now – between 1984 and 1989 – and involved three individuals primarily: Fred Bookstein, Colin

*Corresponding author

Email address: n.macleod@nhm.ac.uk (Norman MacLeod)

Goodall, and David Kendall (see Bookstein 1993). All three had interests in geometry and statistics, but only Bookstein had direct and extensive experience with shape-based data-analysis problems in biology. Subsequent to the late 1980s, a number of important conceptual additions to the corpus of GM have been made (e.g., Rohlf and Slice 1990; Rohlf 1993; Mardia and Dryden 1998; Dryden and Mardia 1998), new data analysis methods developed (e.g., the Dryden-Mardia shape test), and methods developed in other contexts applied to morphometric datasets (e.g., machine learning methods, see MacLeod 2008). Nevertheless, from the late 1990s to the present day the main efforts of morphometricians have been spent in introducing individuals to the concepts of GM and applying these concepts to various problems in comparative morphology, or anatomical, analysis (see Adams et al. 2004).

But, does this exhaust the range of contexts appropriate for morphometric intervention? After all, form, and shape are not only important attributes of non-anatomical aspects of biology, they transcend the biological sciences entirely. For example, a host of variables important for managing forests in conservationally responsible and commercially optimal ways can be inferred from image texture analysis (e.g., Roiu and Seyer 1997; Franklin et al. 2001; Kayitakire et al. 2006). To date GM-based morphometric methods have not been used to characterize or compare forest canopy textures though in principle this geometric problem does not differ substantially from the characterization of bone or shell surface textures in biological species. Mechanistically, correct geometric design of the surfaces of the receptor cells responsible for the senses of taste and smell is as important (if not more so) than the ability of these receptors to respond to the presence of various chemical species (Young, 2001; Cramer, 2004). The tools of GM could, in principle, assist with the quantification and design of molecules that match molecular receptor surfaces. And while sound often has quite a complex structure, any digitized sound can be represented as a shape and so be subjected, in principle, to GM analysis.

To date GM has not been employed either extensively or routinely in any research field outside that of comparative anatomy/morphology. But this only means that the utility of GM approaches to the study of phenomena that represent the subject matter of these fields remains unexplored. In the past extra-anatomical applications have been limited because the nature of the shapes these phenomena present differ markedly from the anatomical/morphological structures that are well understood by morphometricians from the standpoint of shape characterization. In particular, many of these non-traditional shapes are best characterized as continuous two-dimensional (2D) functions or three-dimensional (3D) surfaces that do not appear to lend themselves to appropriate characterization using a small set of topologically homologous landmarks (see Aston et al. 2012). However, as the semilandmark – once all but excluded from consideration as an adequate morphometric descriptor (e.g., Bookstein 1990, 1991) – has now been rehabilitated as a useful implement in the morphometrics toolkit, and as semilandmark-based sampling protocols have been developed to facilitate the analysis of heretofore "featureless" surfaces (see Bookstein 1997; MacLeod 1999, 2008, 2012; Adams et al. 2004; Gunz et al. 2005; Polly 2008; Polly and MacLeod 2008; Klingenberg 2008; Oxnard and O'Higgins 2008; Sievwright and MacLeod 2012), the conceptual gaps between extra-anatomical objects and the sorts of forms GM is used to analyze, routinely seems less formidable now than they once did.

In order to explore the contribution GM can make to the analysis of non-traditional form, this contribution will focus on the analysis of sound; specifically the geometric analysis of bat echolocation calls. Some bats, along with odonocetes (toothed whales & porpoises), some birds (oilbirds, swiftlets), and some terrestrial mammals (shrews, tenrecs, even humans to a limited extent – see Supa et al. 1994; Thaler et al. 2011 for a discussion) use acoustic echolocation to navigate through, and identify objects in, their environment, though this capability is better developed in bats than any other organismal group.

Bats typically emit calls in the frequency range from 14.0 kHz to over 100 kHz; well outside the sensitivity range of human audio reception (9 Hz – 212 kHz). Bat calls are known to have a significant association with habitat, sex, age and presence of con–specifics in terms of dif-
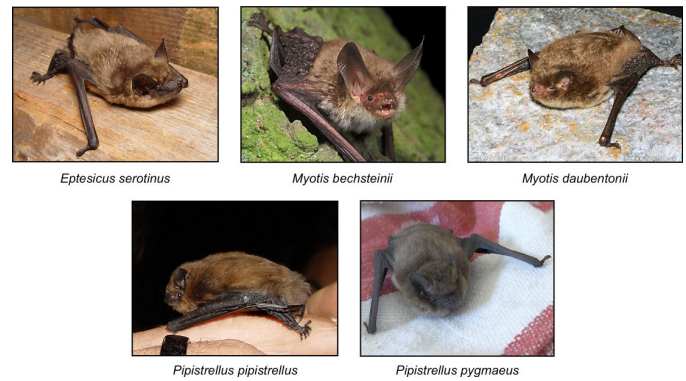

Eptesicus serotinus   *Myotis bechsteinii*   *Myotis daubentonii*

Pipistrellus pipistrellus   *Pipistrellus pygmaeus*

Figure 1 – Bat species used as the primary subjects of this investigation.

ferent types of calls being used for different purposes. When hunting, bats use different calls to locate, identify, track, and intercept different types of prey. Different types of calls are also used in different locations though, if possible, a bat will prefer to hunt in an area for which its call type is suited (see Schnitzler and Kalko 2001). For these functional reasons bat echolocation calls are known to be species specific as well as diverse. This latter attribute raises the possibility of designing automated systems to identify bat species remotely by analysing the characteristics of their calls. If call-based remote identification can be realized on a sufficiently large scale, and with sufficient accuracy, it would be of great importance to bat conservation efforts as bats themselves are difficult to catch, especially without causing physical harm to the individual. Bat calls are able to be recorded using microphones, but such recordings are only accurate at present if expensive audio sensors are used. There is even an app – iBat – for iPhone and Android operating systems that will allow smart phones to be used as bat call recording devices and to upload the recorded calls to a central repository at the Institute of Zoology, London where software can assist in identifying the call (http://www.ibats.org.uk). If robust automated algorithms for identifying bat species from the physical attributes of their call patterns can be realized, the efforts of a growing cadre of committed and enthusiastic citizen scientists could be enhanced to provide reliable census data in the cause of promoting bat biology/ecological research and bat conservation efforts (Jones et al., 2013).

Accordingly, the goals of this investigation are fourfold.

i) Description of a generalized, geometry-based strategy for analysing bat search phase echolocation calls quantitatively that takes advantage of GM concepts and tools.

ii) Comparison and contrast of results obtained using this new morphometric approach to acoustic signal analysis with more traditional approaches.

iii) Discussion of avenues and opportunities for future research that might be pursued in the context of a shape analysis-based approach to the analysis of bioacoustic signals.

iv) Encouragement to (a) morphometricians to expand the scope of their work beyond the routine analysis of physical morphology and (b) non-morphometricians to realize and appreciate the potential of geometric approaches to contribute directly to testing what have traditionally been regarded as non-morphology-based hypotheses in their field(s) of study.

Materials and methods

For the primary example dataset a sample of calls from five bat species (Fig. 1) was obtained from the EchoBank bat call archive, a bat call reference library hosted by the Zoological Society of London. These species are all known to occur in the UK. Twenty calls were selected from each species at random in order to obtain a model of within-species call variation. In addition to this a second set of EchoBank calls was collected from bats belonging to the genus *Myotis*, which is regarded as a challenging group to identify to species level from echolocation call signatures alone (Kalko and Schnitzler, 1993; Parsons and Jones,
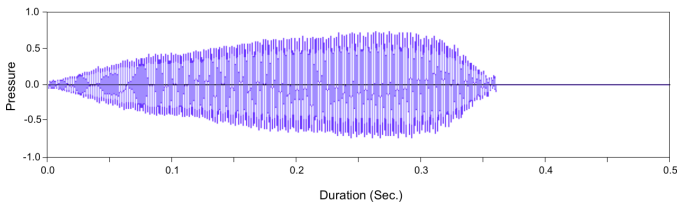
Figure 2 – Raw (non-normalized) oscillogram for a typical *Pipistrellus pipistrellus* search call. This call has a duration of 0.36 sec. and a maximum volume of 0.62 pressure units.

Spectrograms are constructed from oscillograms by applying a Fast Fourier Transform (FFT) to these amplitude vs. time data to represent or re-describe the complex waveform as a series of frequencies with associated frequency amplitudes. A sound file that has been re-expressed as a Fourier series of frequencies is said to have been transformed into the "frequency domain". A plot of a sound's structure on a graph of amplitude vs. frequency is often referred to as a "power spectrum".

Finally, a 3D representation of the sound can be obtained using a sampling window that breaks the sound into chunks composed of an equal number of data points; usually some power of 2 (2^2, 2^4, 2^8, 2^9, 2^{10}), a convention that derives from the mathematics of the FFT. These windows are moved down the signal by a specified amount, termed the "offset" (usually another power of 2, but one that is less than the window length), so that successive windows overlap by a constant amount. A FFT of the data included in each window is calculated and the associated amplitudes recorded as a matrix of numbers with the rows of the matrix representing the number of windows or chunks and the columns representing the number of frequency harmonics used to describe the sound included in each window. Of course, since the number of points included in each window is the same, the number of frequency harmonics extracted from each window will be the same. This procedure is referred to as a short-time or "windowed" Fourier analysis.

One complication inherent to the windowed approach is it will rarely be the case that the first and last point within each windowed dataset will have the same amplitude value. If this is not the case the Fourier decomposition procedure will artificially assign a high amplitude to a high-frequency harmonic. The most commonly employed procedure to correct this problem is to multiply every point in the raw (windowed) dataset by a continuous weighting function that, in effect, forces the ends to adopt the value 0.0 while not inducing distortion in the central section of the sound segment. A number of different weighting (or window) functions have been developed for this purpose including the Hanning, Hamming, Blackman, Bartlett, Turkey, and Laczos functions (see Harris 1978).

Typically, the set of variables resulting from a windowed Fourier analysis – call duration, set of harmonic frequencies, and amplitude values associated with each frequency for each windowed chunk of the sound – are assembled into a 3D image of sonic structure. These "spectrograms" have long been used to represent and compare both human and animal vocalization patterns. Spectrograms of this general form have been referred to variously as spectral waterfalls, sonograms, voiceprints or voicegrams. An example of a Hanning windowed call frequency spectrogram for a typical bat echolocation call is shown in Fig. 3. The 3D structure of the call is usually represented as a colour-
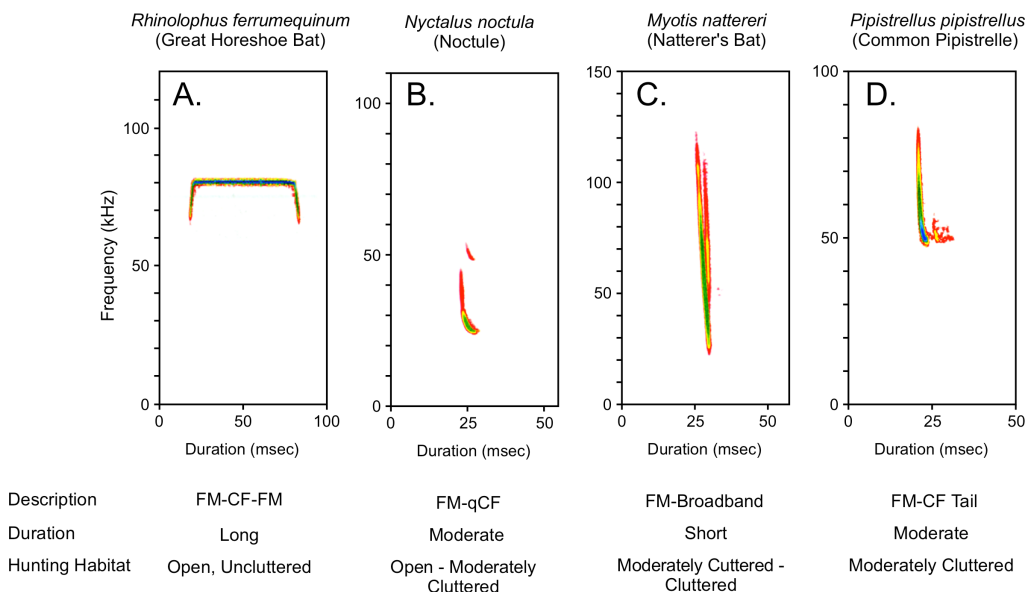
2000; Lundy et al., 2011). Nine *Myotis* species were used for this part of the analysis: *M. bechsteinii*, *M. blythii*, *M. brandtii*, *M. capaccinii*, *M. daubentonii*, *M. emarginatus*, *M. myotis*, *M. mystacinus*, and *M. nattereri*. Each of these species was represented by ten calls.

The calls themselves were full-spectrum, digital audio recordings of bat detection or search calls (as opposed to feeding buzzes or social calls) recorded at a sampling frequency of 44.1 kHz. These calls were obtained as primary digital audio recordings and saved to disk in the Microsoft .wav file format. Although each recording contains multiple calls from a single individual, only one was selected for analysis in this investigation. Minimal processing was applied to each call to standardize its structure. This processing procedure consisted of (1) normalizing the amplitude of each call to standardize its volume and (2) editing each call file to ensure it encompassed an equivalent total duration. The latter step was accomplished by determining the duration of the longest call in the sample and padding the ends of the shorter calls with silence taking care to make certain that each call began at the first position in the file listing. This step is necessary to ensure that each call can be compared across the sample in a reasonable manner and to verify that each call will be represented by the same number of geometric variables (see below).

Currently there exist three approaches to the quantitative analysis of bioacoustic signal data generally and bat echolocation calls in particular (Russ, 2012). The primary method of data collection quantifies the sound wave as a series of pressure readings taken at equal time intervals during the course of the call. A graph of these data that plots sound amplitude (= energy) against time is termed an oscillogram (Fig. 2). Oscillograms have been used to study many aspects of sound and are familiar to many musicians and fans of digital music, as well as acoustic researchers, from the graphical displays of digital sound editing software.

	Rhinolophus ferrumequinum (Great Horeshoe Bat)	*Nyctalus noctula* (Noctule)	*Myotis nattereri* (Natterer's Bat)	*Pipistrellus pipistrellus* (Common Pipistrelle)
Description	FM-CF-FM	FM-qCF	FM-Broadband	FM-CF Tail
Duration	Long	Moderate	Short	Moderate
Hunting Habitat	Open, Uncluttered	Open - Moderately Cluttered	Moderately Cuttered - Cluttered	Moderately Cluttered

Figure 3 – Representative bat spectrogram call forms with their standard qualitative descriptors (description, duration) and typical hunting habitat. Abbreviations: FM – frequency modulated, CF – constant frequency, qCF – quasi-constant frequency. Redrawn from Russ (2012).
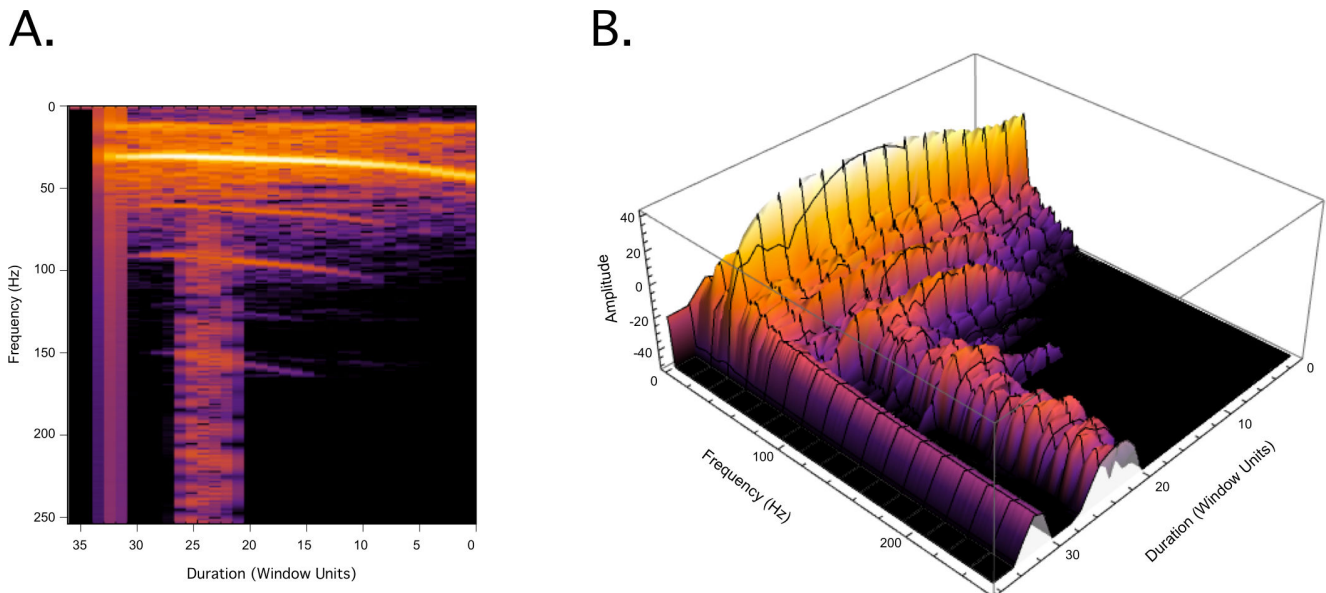
A.

B.

Figure 4 – Hanning windowed spectrograms for the *Pipistrellus pipistrellus* search call shown in Fig. 1 after normalization and padding to extend it to boundary of the oscillogram sampling window. The spectrogram is shown as a color coded 2D matrix (A) and an interpolated 3D surface (B). Note that the bright (yellow-white) band marking the fundamental harmonic sweep in (A) corresponds to the prominent ridge of amplitude values in the 3D surface representation (B) of the call's structure.

coded topological plot of call duration and harmonic frequency with amplitude values represented as a greyscale or color region mappings (e.g., see Schnitzler and Kalko 2001; Teeling 2009; Russ 2012; Fig. 3).

The traditional approach to using of spectrograms to achieve a quantitative description of acoustic signal structure in a manner that lends itself to qualitative analysis has been to employ a rather small number of observations and/or simple descriptive terms that capture a very limited subset of the spectrogram's overall geometry (see Russ 2012 and Fig. 3). Nonetheless, using these data, in addition to visual inspection of the spectrogram patterns themselves, it has been possible to determine that, as a group, bat species have evolved differently structured calls to take advantage of, or to compensate for, physical features of their preferred hunting environments and preferred prey items. For example, bats that hunt in open spaces utilize long duration, constant frequency (Fig. 3A) or quasi-constant frequency (Fig. 3B) calls that achieve maximum range with low atmospheric attenuation (Schnitzler and Kalko, 2001; Teeling, 2009; Russ, 2012). In contrast, bats that hunt in spatially complex, cluttered environments tend to utilize either short-duration, broadband, linear frequency modulated calls or short-duration, broadband, linear period modulated calls to sense the structure of their surroundings (Fig. 3C and 3D). Many bat species also rely on a variety of additional strategies for prey detection (e.g., auditory cues, Doppler shift, see Fenton et al. 1995; Jones 1999; Schnitzler and Kalko 2001). Finally, species that hunt in edge or mixed environments tend to utilize calls with both constant frequency and frequency modulation components with a relatively longer, narrow bandwidth, quasi-constant frequency character to achieve both localization sensitivity and high detection performance (Schnitzler and Kalko, 2001).

Over and above this generalized relation of call sonic structure to the physical aspects of different hunting environments, representation of bat search echolocation calls by means of a spectrogram can support, in a general sense, the testing of a variety of functional, ecological, and phylogenetic hypotheses. It does this in the same way that morphological features of anatomy support the same sorts of investigations, including phylogenetic analyses. For example, it is already known that, in many bats, call type is consistently associated with differences in homologous anatomical characters (e.g., length, width, and shape of the wing). This should not come as a surprise because, even through the concept of biological homology cannot be applied to acoustic structures *per se*, there is an obvious functional relation between the physical capabilities of particular (say) wing designs with regard to characteristics of the environment in which flight takes place and the type of au-

dio signal best suited for echolocation duties in that same environment. Therefore, provided methods for representing the complex structure of these calls can be developed, it should be the case that morphometric approaches can be applied to the characterization, comparison, and analysis of these "non-morphological" structures in the same way they are applied to morphological structures.

For this investigation all calls were placed within an interval of 0.1023 seconds, which yielded call files 4512 sample values in length. This is equivalent to representing each call as a 4512-dimensional column vector. All calls were set to begin at time = 0.0 (sample = 1). Beyond normalization of the call amplitude and padding of the call duration, no filters were used to "clean" (e.g., sense or eliminate acoustic reflections from nearby surfaces) or enhance the sound. While on occasion reflections from certain surfaces can be helpful in bat identifications (e.g., bats that hunt over water, see Russ 2012), identification using acoustic signals generated by the bat itself is usually preferable.

While it has been the case to date that sonic spectrogram data have been characterized by and described on the basis of the 3D color-coded contour maps such as those shown in Fig. 3, these data can just as easily – and arguably more accurately from the standpoint of quantitative form characterization/comparison – be represented as true 3D elevation plots (see Fig. 4). Accordingly, sonic spectrograms were calculated from each call oscillogram in order to represent its form as a 3D surface. A spectrogram chunk size of 512 data points, with a chunk offset of 128 data points, was chosen to order to construct the window which also employed the Hanning function to minimize the amount of frequency leakage that occurs as a result of the chunked signal segments being non-continuous. These are standard spectrogram window settings.

This calculation resulted in a representation of each call as set of 36 chunks each of which was 512 samples long with each chunk being described by 512 Fourier harmonic amplitude values. Note this is a complete Fourier spectrum. To avoid redundancy due to aliasing all analyses were confined to the unique portion of the Fourier spectrogram (see Fig. 3). Once conversion to the windowed spectrogram had been accomplished for all calls amplitude values less than an arbitrarily chosen cut-off value of -50 were reassigned that value in order to provide a limit against which to distinguish between the call signal and background "noise". In terms of the shape of the call structure this background establishes the duration and frequency attributes of each call's form. This background normalization is a standard signal-processing technique (see Russ 2012) and, in a sense, is the sonic equivalent of placing a specimen on a black background prior to collecting a

digital image of its form. Exploratory experiments showed that above the -50 value results of the analysis changed markedly depending on which background normalization cut-off level was chosen, but below this level results were remarkably constant.

Redescription of the bat call oscillograms as Fourier-transformed sonic spectrograms increased the dimensionality of the call form from 4512 values to 8960 values, with this increase resulting from the fact that each window chunk is described by 256 unique harmonic amplitudes. This procedure resulted in a highly-detailed, but also highly redundant, representation of the each call's physical structure. Such redundancy can be minimized, and the major features of the call structure preserved for analysis, by mathematically laying a call-sampling grid over the windowed call and recording only the duration, frequency, and amplitude values that occupy the nodes of the sampling grid. This represents a surface-shape sampling system analogous to that used in eigensurface analysis (MacLeod, 2008; Sievwright and MacLeod, 2012) for which object size (here represented by call duration) has been included for an identical purpose: to represent the geometry of a highly

variable, but consistent, featureless surface accurately and efficiently as a set of topologically homologous semilandmarks that bear a consistent geometric relation to each other and to the underlying "morphology" – in this case the windowed spectrogram. Gunz et al. (2005) utilized a similar semilandmark-based phenetic procedure to analyze the shape of the cranial vault in humans though the grid sampling procedure used in eigensurface analysis is both more structured and applicable to a greater diversity of forms. Specification of grid dimensions provides analysts control over the fidelity of the call's spatial – and so acoustic – representation. Coarse sampling grids will capture only the gross call form whereas finer grids will preserve greater levels of sonic detail. Using this strategy there is even scope for automating the spectrogram-sampling process so that analysts can be sure all grids sample the spectrogram to a consistent minimum quality criterion (see MacLeod 1999 and MacLeod 2008 for a discussion in the context of eigenshape analysis and eigensurface analysis respectively). Figure 5 shows results for a series of sub-samplings of the *Pipistrellus pipistrellus* spectrogram shown in Fig. 3 using square sampling grids of 10, 15, 25, and 35 cells per side. Note the rapid convergence on a reasonably detailed estimate of raw spectrograph shape both in terms of call feature shape and call feature location even at what would be considered coarse grid resolutions. In this study either a 30-cell (mixed bat genera dataset) or a 25-cell (*Myotis* species) grid was used to represent the generalized aspects of bat call structure. This level of detail was was judged (via visual inspection) to contain all the key features of the original spectrogram (compare Fig. 5 with Fig. 4). Selection of this resolution means that each spectrogram was described by 900 variables. Of course, this is still a very high-dimensional dataset. But in fact these data represent only 20 percent of the original spectrogram data; a considerable reduction in the dimensionality of the original dataset.

Sampled in this way the spectrogram data are, effectively, shape data that reside as point locations on a high-dimensional ($n = 900$) Kendall shape manifold. The 30-cell grids that were mathematically superimposed over the spectrogram surface are topologically homologous across the dataset in the sense that each grid point bears a consistent spatial relation to all other points on the grid. Indeed, the duration and frequency coordinates of all grid nodes are identical across all spectrograms in the subsampled dataset; only the amplitude values vary. As is standard practice in geometric morphometric investigations, these amplitude data were re-expressed as deviations from the mean spectrogram shape for the pooled sample (Fig. 6). Re-expression of the spectrogram data in this manner allows the acoustic structure of the search call sounds to be represented in a rigorous and fully quantifiable manner as shapes. Once these grid-based samplings of the original spectrogram data are in this form they can be operated on by all the procedures of geometric morphometrics.

For this investigation a preliminary covariance-based principal components analysis (PCA) was carried out on the pooled bat call spectrogram shape dataset in order to reduce the effective dimensionality of the dataset still further. This step is also important for assessing the major directions of shape (= call) variability for the sample and for serving as a basis space for call modeling procedures that will be used to interpret the placement of call groups in a linear projection space derived from the Kendall shape manifold. Results of the PCA analysis were used to decide how many latent shape variable axes to retain for subsequent discriminant analysis. The decision criterion for this phase of the investigation was to retain call configuration scores on a sufficient number of eigenvectors to ensure that at least 95 percent of the observed call-shape variability was retained for subsequent group-based analyses.

To serve the needs to rhetorical brevity, these data analysis steps – including (1) calculation of the Hanning windows, (2) subsampling of these windows based on grids of user-specified dimensions, and (3) summarization of major trends in acoustic structural variation via ordination of the positions of spectrogram surface shape coordinates in a reduced PCA subspace – will henceforth be referred to as "eigensound" analysis. This term is simply a convenience that streamlines procedural and interpretive descriptions and discussions in much the same way that

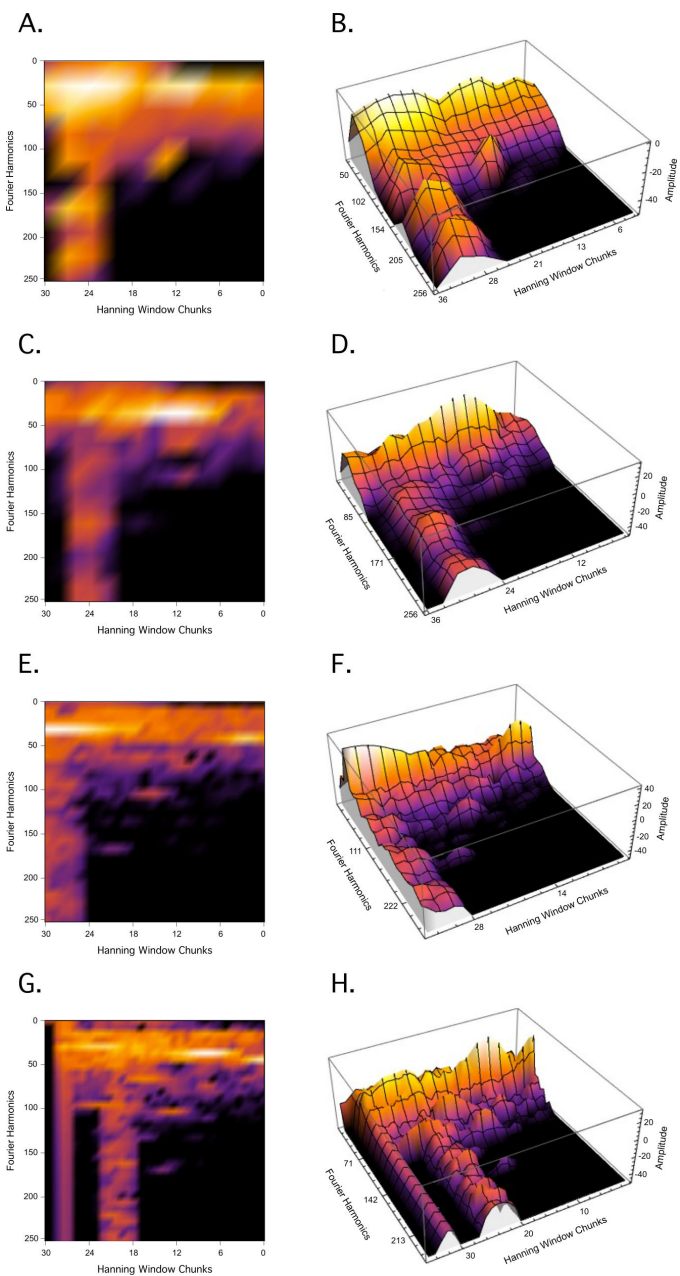**Figure 5** – The effect of choosing different subsampling grid resolutions on the character of the estimated spectrogram. Compare each down-sampled *Pipistrellus pipistrellus* spectrogram with the full-resolution *Pipistrellus pipistrellus* spectrogram shown in Fig. 3. For the purposes of the analyses of the primary bat call dataset a square grid resolution of 30 cells per side (900 cells in total) was chosen.
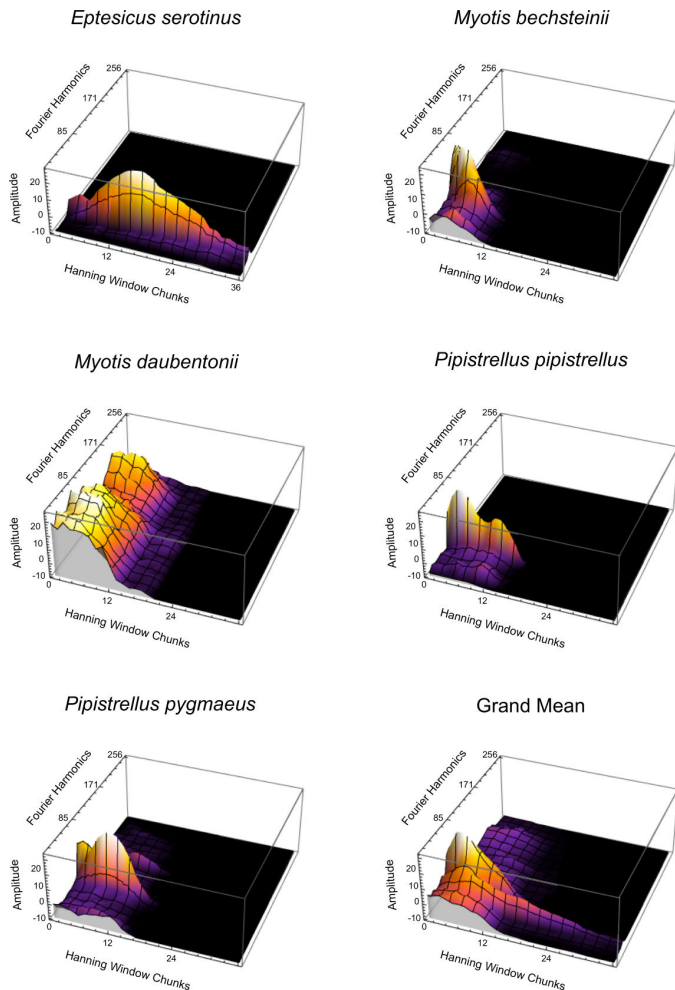
Figure 6 – Mean search call spectrograms for the five bat species included in the primary call dataset along with the grand mean for the pooled sample.

groups present in that dataset, resulted in the specification of eight discriminant functions. In order to obtain a robust estimate of group discrimination efficiency and address issues arising from the high dimensionality of the eigensound dataset both standard CVA and Monte Carlo CVA (see Manly 1997) procedures were employed.

Geometric interpretation of the CVA space was facilitated through the calculation of along-axis shape models using the back-projection procedure presented originally in MacLeod (2009a) and used in a number of recent articles (e.g., MacLeod 2008; Bolton et al. 2008; Sievwright and MacLeod 2012). Statistical tests of the separation between-group centroids in the CVA space relative to within-group dispersion of the data were carried out using the log-likelihood ratio (Φ) method for which the probability (ρ) of obtaining observed differences between sample mean vectors can be determined via reference to the χ^2 distribution (see Manly 1994). Both efficiency and stability of the discriminant functions calculated on the basis of call geometry were also tested using both the raw training set data and a jackknifed CVA.

Finally, in order to compare and contrast results obtained using a geometric approach to bat echolocation call analysis a set of standard call-description variables was obtained by Collen (2012) using SonoBat software from the EchoBank archive. Tab. 1 lists the variables included in that reference dataset. These variables were used by Walters et al. (2012) as the subset of possible descriptors that are most useful for quantifying between-taxonomic group distinctions between call types. To ensure strict comparability of results, these traditional spectrogram descriptor data were subjected to the same data-analysis procedures as the eigensound data.

Results

Inspection of mean spectrograms for the initial five-species dataset (Fig. 6) provides evidence for pronounced species-specific differences in call form. *Eptesicus serotinus* exhibited the most divergent call pattern, a long duration call with a narrow bandwidth focused into a prominent low-frequency fundamental harmonic. This pattern is typical of a high duty-cycling call, often employed by species hunting in open uncluttered environments. In contrast the two *Myotis* species are characterized by comparatively short, low duty-cycling calls with pronounced low-frequency energy peaks that may (*M. daubentonii*) or may not (*M. bechsteinii*) exhibit frequency modulated mean call shapes. *Myotis* species typically hunt in cluttered environments and/or over water (*M. daubentonii*). The two *Pipistrellus* species exhibit calls with their own structural differences. The *Pipistrellus pipistrellus*' mean call exhibits the short-to-intermediate duration and narrow bandwidth typical of species that hunt in marginal, semi-cluttered environments whereas the *Pipistrellus pygmaeus* mean call exhibits a form of similar duration, but longer bandwidth (especially at higher frequencies) and a marked difference in peak-amplitude profile. Both these species exhibit a prominent low-frequency fundamental harmonic, but the former is unique in its possession of a well-defined, subsidiary, higher-frequency secondary harmonic ridge.

The pooled sample mean shape (Fig. 6, lower right corner) represents a complex amalgam of these singular patterns. This mean is an abstract mathematical concept that corresponds to the call pattern of

the terms "Procrustes analysis", "principle warps analysis" and "relative warps analysis" function in the standard GM literature. "Eigensound analysis" was chosen to highlight the conceptual links between this geometry-based approach to acoustic signal surface analysis and its morphological equivalents: eigenshape analysis (Lohmann, 1983; MacLeod, 1999) and eigensurface analysis (MacLeod, 2008; Polly and MacLeod, 2008; Sievwright and MacLeod, 2012).

Once the secondary data matrix of PC scores had been assembled, these data were combined with a grouping variable that associated each set of PC scores with the species name of the caller, and the dataset submitted to a canonical variates analysis (CVA, see Campbell and Atchley 1981; MacLeod 2007). Since five species were present in the primary sample test data, four discriminant functions were calculated and used in subsequent investigations. The *Myotis* dataset was treated in an identical manner which, owing to the larger number of species

Table 1 – Traditional bat echolocation call descriptors.

| Variable Name	Description
LowFreq	Minimum frequency of the call (kHz)
FreqMaxPwr	Frequency of the call at the point of maximum amplitude (kHz)
HiFreq	Maximum frequency of the call (kHz)
Bndwdth	Bandwidth: total frequency spread of the call, calculated from the difference between maximum and minimum frequencies of the call (kHz)
CallDuration	Duration of the call (ms)
FreqCtr	Frequency at half the duration of the call (kHz)
Fc	Characteristic frequency: frequency of the instantaneous point in the final 40% of the call with lowest slope (kHz)
FreqKnee	Frequency at which the initial slope of the call most abruptly transitions to the slope of the body of the call (kHz)
FreqLedge	Frequency of the most extended flattest slope section of the call preceding the characteristic frequency (kHz)
StartSlope	Slope in the first 5% of the call duration (kHz/ms)
SteepestSlope	Steepest slope of the call: the maximum of linear regressions of any segment of 10% of the duration of the call (kHz/ms)
HiFtoKnSlope	Slope of the call calculated from the frequency and time of the point of highest frequency to the frequency and time of the knee (kHz/ms)
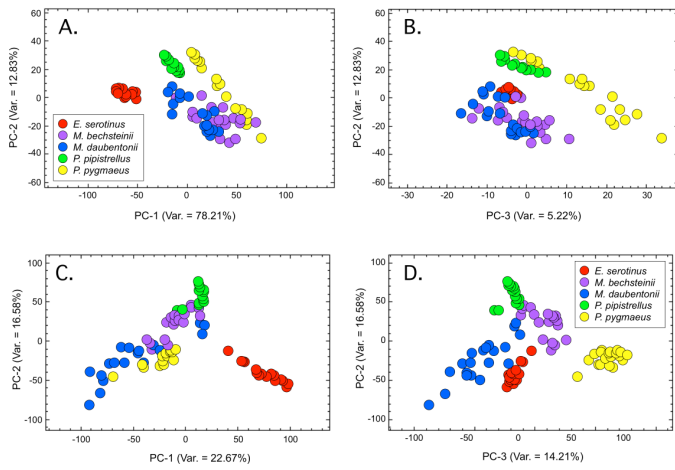
Figure 7 – A.-B. Distribution of bat species call geometries in the subspace formed by the first three principal components of correlation matrix calculated from 12 traditional spectrograph descriptors. C.-D. Distribution of bat species call geometries in the subspace formed by the first three principle components of a 30-cell sampling grid-based representation of spectrograph shape coordinates. Note differences in the axis scales which have been adjusted to save space. See text for discussion.

no known bat species, ancient or modern. Nevertheless, it plays an important role in the analysis as it specifies the semilandmark point configuration that locates the optimal set of linear planes tangent to the Kendall shape manifold on which to project the actual call configurations in order to visualize the structure of shape relations among them.

Principal Component Analysis – Traditional Spectrogram Variables

To establish a baseline against which the performance of an eigensound approach to acoustic spectrogram characterization and analysis can be evaluated, results obtained via application of this method were compared to results obtained from a mathematically comparable analysis of a series of 12 traditional spectrogram variables typically used to assess the structure of spectrogram similarities and differences in call echolocation studies across the a sample of the same five species that comprised the primary dataset (see Walters et al. 2012). These data represent observations of interest with respect to the characterization and comparison of spectrogram-based representations of acoustic data (e.g., maximum recorded frequency, bandwidth). They are not geometric in the sense of making any systematic attempt to represent the form or shape of the call spectrogram in any but its most generalized aspects. Nevertheless, it is these types of variables that are used at present to quantitatively characterize all bat echolocation calls (see Russ 2012).

As a first step in analyzing these traditional spectrogram data a PCA was performed to make a preliminary assessment of the datasets' major axes of variation and, if appropriate, reduce its dimensionality by focusing the spectrogram shape information distributed across all raw variables into a smaller set of composite, or latent, variables. Because the units associated with the traditional spectrogram variables differ from one another a correlation (rather than a covariance) matrix was used to assess the between-variable structure of these data.

Figures 7A-B shows the subspace formed by projection of the raw data values onto the first three eigenvectors of the correlation matrix calculated from this traditional spectrogram descriptor variable set. This subspace represents 96.3 percent of the observed variation described by the set of traditional variables. Although the point clouds for all species except *E. serotinus* are distributed over relatively large regions, three of the five species occupy unique domains within this subspace. The two *Myotis* species' domains overlap strongly, a result that is consistent with previous reports of difficulties separating *Myotis* species on the basis of their call patterns as assessed by traditional spectrogram descriptors (Vaughan et al., 1997; Parsons and Jones, 2000; Walters et al., 2012). Interestingly, whereas *E. serotinus* calls project to uniformly low positions along PC 1, the extremes of PC 2 and PC 3 are occupied by multiple groups. This result suggests that, with the ex-

ception of the *E. serotinus*, between-groups variation is not well aligned with the major axes of call form variation in the pooled dataset. Nevertheless, the scatter of points in the subspace these three eigenvectors indicates that these traditional variables do capture important aspects of within-species similarity and between-species differences.

Inspection of the eigenvector loadings for these axes indicates that calls plotting low on PC 1 are characterized by relatively high minimum frequencies, a high frequency that represents the transition from the initial phase and the body of the call, low maximum frequencies, and low frequency slope gradients. Calls that plot high on PC 1 exhibit the opposite characteristics and trends. Along PC 2 calls that project to low positions are characterized by low amplitudes, low bandwidths, high ledge frequencies and high frequency gradients whereas calls that project to high positions along this axis are characterized by high call amplitudes, high bandwidths, low ledge frequencies and low frequency gradients. Calls that project to positions low on PC 3 possess high ledge frequencies, high frequency gradients, low maximum frequencies, and low bandwidths whereas those that project to high positions are characterized by low ledge frequencies, low frequency gradients, high maximum frequencies, and high bandwidths. Note that, despite the apparent specificity of these spectrogram differences, it is quite difficult to form an intuitive impression of exactly what aspects of these parameters are responsible for the broad range of species-specific call variation domains, characteristic differences in species' call variation patterns, and the between-species distinctions in call form as expressed in this ordination of call structure data. In essence, these traditional variables are either too generalized or too idiosyncratic with respect to the structure of call variation to yield a detailed yet easy-to-visualize result, and the loading patterns too complex to allow for simple and clear interpretations of the PCA space geometries.

Principal Component Analysis – Spectrogram Co-ordinates

As noted above, a covariance-based PCA of the eigensound dataset was also used to assess the major directions of call variation as the final step in an eigensound analysis. The primary purpose of this procedure was to assess dominant patterns of call structure variation and further reduce the dimensionality of the spectrogram structure dataset by focusing the information content of grid-based sampling procedure into a small number of composite, uncorrelated variables. Figures 7C-D show the ordination of call geometries within the subspace formed by the first three eigensound PC axes. Together these axes represent 75 percent of the observed spectrogram surface shape variation.

This ordination of call geometries based on the 3D spectrogram surface shape shows unexpected structure with a suggestion of a classic horseshoe pattern in the plane formed by the first two PC axes (Fig. 7C). The presence of this pattern in the PCA result indicates the existence of a non-linear gradient in these acoustic data. Since this is the first investigation (to our knowledge) that has operated on acoustic spectrogram data using sonic semilandmarks, it is unclear whether such gradients are common in these types of data or whether this is an idiosyncratic feature of this particular dataset. If non-linear gradient-like trends are common in acoustic spectrogram shape data their analysis my require methods specifically formulated to handle such data (e.g., non-linear PCA, kernel PCA, machine learning approaches; see Kramer 1991; Schölkopf et al. 1998; Friston et al. 2000; Scholz et al. 2007).

With respect to linear data analysis, specialists are of two minds regarding the "issues" posed by the horseshoe pattern. Ecologists tend to regard its presence as problematic and have developed a variety of *ad hoc* transformations to eliminate it from their datasets (e.g., de-trended correspondence analysis, see Pielou 1984; Hammer and Harper 2006). Unfortunately, employment of these algorithms runs the risk of obscuring other aspects of the data pertinent to its interpretation. In this context it should be remembered that the horseshoe pattern is always an accurate portrayal of the nonlinear pattern of the data, albeit in a linear space. Most mathematically inclined commentators advocate retention of the horseshoe pattern in the data – its removal is usually justified
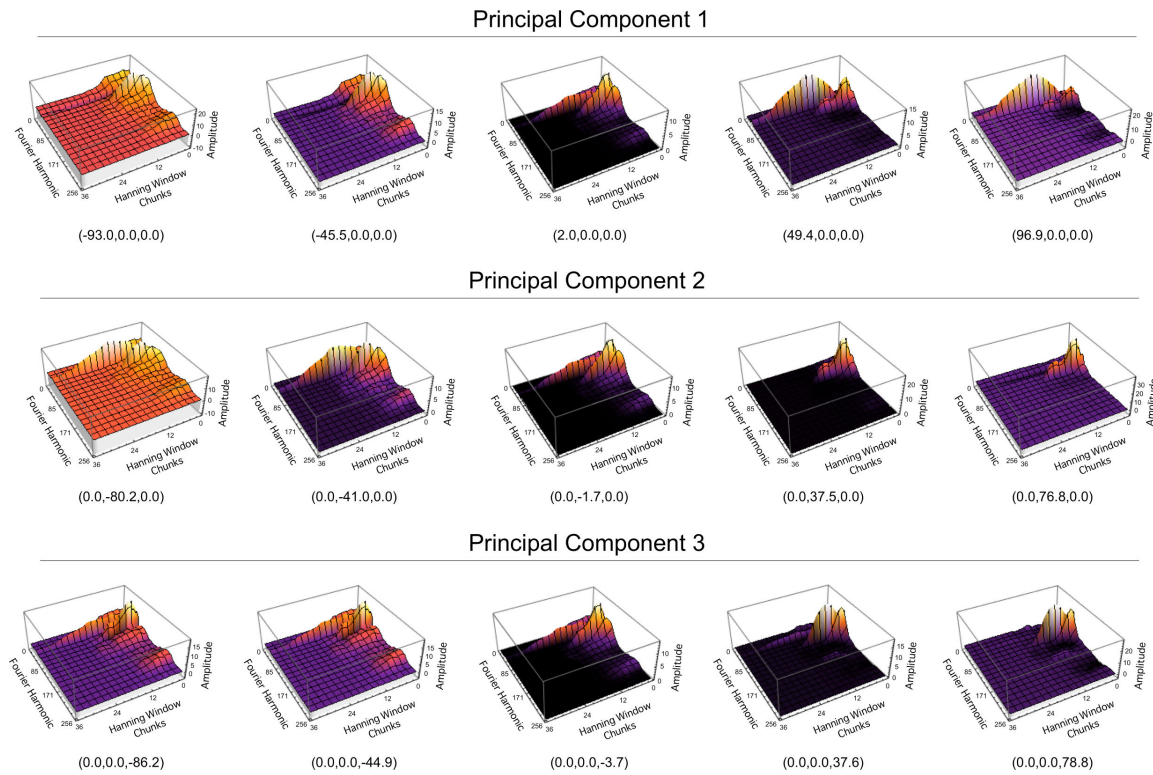
Figure 8 – Hypothetical models of search call shape at a series of equally spaced coordinate positions (listed below each plot) along the first three PC axes. These models provide a visual aid for developing interpretations of the PCA space shown in Fig. 7. See text for discussion.

primarily on aesthetic grounds – while being mindful of its proper interpretation or migrating to a non-linear data analysis procedure if the situation warrants it (see Greenacre 1984; Reyment 1991; Reyment and Jöreskog 1993; Podani and Miklós 2002; MacLeod 2006). Since the purpose of this analysis is to determine whether bat species can be identified by the geometry of their echolocation call patterns, and since the call configuration point distributions along the first two pooled-sample PC axes exhibit a high degree of species-specific clustering, recourse to de-trending algorithms or non-linear variants of PCA was deemed unnecessary.

Unlike the traditional spectrogram descriptor variable results (see Fig. 7A-B), in the eigensound PCA space the extremes of shape variation tend to be occupied by single species groups (Fig. 7C-D). For example, PC 1 represents a contrast between *M. daubentonii* (low scores) and *E. serotinus* (high scores); high scores along PC 2 tend to be dominated by *P. pipistrellus* and *M. bechsteinii*, with *P. pygmaeus* dominating the high end of PC 3. To be sure, some apparent overlap between species groups does characterize this subspace and group-level outliers are by no means uncommon. However, alignment between the major axes of pooled sample shape variation and the primary 3D surface structure-based distinctions in the species' call spectrograms is much greater for the eigensound variables than it was for the traditional set of spectrogram descriptor variables; especially for the acoustically challenging *Myotis* species.

Along PC 1 the two most divergent call geometries are those of *M. daubentonii* and *E. serotinus*. Since the former is the species with the longest mean call duration and the latter the species with the shortest, this would suggest to many that PC 1 represents a call-duration axis. Nonetheless, close inspection of the ordering of group centroids along PC 1 is inconsistent with this simplistic interpretation.

One of the advantages of choosing a geometric approach to acoustic spectrogram analysis is that it is a relatively easy matter to calculate the shapes of spectrograms for any point location on the Kendall shape manifold. This capability is in keeping with the fundamental theory that underlies all Kendall space shape analyses – that each point in the shape space corresponds to a unique configuration of landmark – or, in this case, semilandmark – points. Figure 8 shows a set of five hy-

pothetical spectrogram point configurations that illustrate the manner in which call structure changes along each of the first three eigensound axes. This set of shape models can be used to understand the detailed geometric nature of the ordination space shown in Fig. 7C-D and refine the biological interpretation of the ordinated points therein.

Hypothetical spectrogram shape models for the first eigensound axis (PC 1 of the pooled search call dataset) indicate call semilandmark configurations that plot low on this axis represent, short duration, multi-modal frequency modulated call shapes that exhibit two distinct, relatively high amplitude, but low frequency energy peaks and a low amplitude, but broader high-frequency amplitude peak. This model matches the mean representation of *M. daubentonii* well (compare with Fig. 6). With movement in a positive direction along the eigensound axis 1 the call shape changes in three ways: call duration is increased, the low-frequency amplitude ridge of high call energy splits into two (biharmonic) sharply defined, low frequency ridges with high frequency components of the call becoming progressively less well-defined and more attenuated overall.

Because of the influence of *E. serotinus* call shapes on the dataset as a whole, duration plays a strong role in the ordination of individuals along each of the first three eigensound axes, though its effect is most pronounced along axis 1. In this sense then, a naïve, qualitative interpretation of the PC space based on species located at the extremes of the various axes (see above) would be very misleading. These along-axis graphical models show quite clearly that, instead of call duration *per se*, axis 1 actually captures the contrast between low duty cycling, frequency modulated calls with a moderate and broadly defined low-frequency energy peak (low scores) and high duty cycling, narrowband, biharmonic calls with sharply defined low-frequency harmonics and attenuation of the call structure at higher frequencies (high scores).

Extending this geometric interpretation to the second and third eigensound dimensions, axis 2 captures the distinction between long-duration calls with low levels of frequency modulation and a pronounced low frequency biharmonic structure (low scores) passing along the axis to calls typified by short durations, high levels of frequency modulation and a sharp, well-defined, linear fundamental harmonic in which the maximum energy level is reached very early in

the call sequence (high scores). Similarly, axis 3 captures the distinction between long-duration calls with a well developed multi-harmonic structure that occupies (discretely) the entire frequency range (low scores) to calls characterized by short-durations and a sharply defined, low frequency, fundamental harmonic structure in which the call's maximum energy is reached early, but extended over the entire initial phase of the call.

When call spectrogram geometries are projected into this subspace species-specific clouds of points are fairly well segregated. Outlying call shapes exist for all these species; particularly so in the cases of *M. daubentonii* and *E. serotinus*. However, the eigensound ordination space is not designed to gather groups together and should not be used to evaluate hypotheses of either group membership or group distinctiveness unless such hypotheses are bound up with assessments of major directions of variation in the pooled dataset. As this is not the case in the present study, these results were used primarily to further reduce the dimensionality of the spectrogram shape characterization problem by focusing the information content of the 900 sampled amplitudes at the sampling grid nodes into a small number of orthogonal variables. Inspection of the table of associated eigenvalues indicated that the first 28 eigenvectors of the pooled-sample covariance matrix capture 95 percent of the spectrogram surface shape variation. Accordingly, the scores on these first 28 eigensound axes, along with a grouping variable specifying the positions of *a priori* groups within the dataset, were assembled and submitted to a CVA. Note this reduction from the 4512 original values in the .wav data files represents a dimensionality savings of 99.6 percent with less than 5 percent loss of geometric information content for this sample. Of course, part of this dimensionality reduction is bound up with the value of n (= number of specimens, in this case 100) which, for most datasets of this type, will always be much less than m (= number of variables, in this case 900). But even if the size of the dataset rather than the number of variables is used as the standard of comparison, a 72 percent reduction in dimensionally with less than a 5 percent loss of geometric information content remains impressive.

Canonical Variates Analysis – Traditional Spectrogram Variables

Although four discriminant axes with positive eigenvalues were specified as a result of the traditional variables CVA analysis, the character of group-optimized separations can be appreciated from an inspection of CV axes 1-3 (Fig. 9). For this variable set *E. serotinus*, *P. pipistrellus*, and *P. pygmaeus* all formed tight, well-separated domains within the CV space. However, the two *Myotis* species exhibited a much wider range of variation along with a substantial overlap in their call form distributions. Again, this result is consistent with the experience of other analysts who have employed a traditional spectrogram descriptor variables, even when these variable sets are analysed by non-linear procedures (e.g., Parsons and Jones 2000; Redgewell et al. 2009; Walters et al. 2012).

Based on results of the log-likelihood ratio test for group centroid separation relative to group dispersion ($\Phi = 638.00$, df = 24), the null hypothesis that these call geometries can been explained by drawing
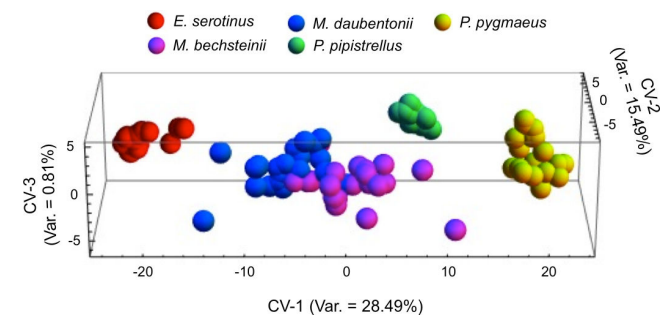

Figure 9 – Distribution of bat species call geometries in the subspace formed by the first three canonical variates of a six-dimensional PC-based representation of traditional spectrograph descriptors. Note differences in the axis scales. See text for discussion.

Table 2 – Confusion matrices for eigensound-based CVA results of call spectrogram form for mixed bat species.

Raw cross-validation identifications of the training set specimens

Species	*E. serotinus*	*M. bechsteinii*	*M. daubentonii*	*P. pipistrellus*	*P. pygmaeus*	**Total**	% Correct
E. serotinus	20					20	100.00
M. bechsteinii		20				20	100.00
M. daubentonii			20			20	100.00
P. pipistrellus				20		20	100.00
P. pygmaeus					20	20	100.00
Total	20	20	20	20	20	100	100.00
% Incorrect	0.00	0.00	0.00	0.00	0.00	0.00	

Jackknifed cross-validation identifications of the training set specimens

Species	*E. serotinus*	*M. bechsteinii*	*M. daubentonii*	*P. pipistrellus*	*P. pygmaeus*	**Total**	% Correct
E. serotinus	20					20	100.00
M. bechsteinii		15	5			15	75.00
M. daubentonii		4	16			16	80.00
P. pipistrellus				20		20	100.00
P. pygmaeus					20	20	100.00
Total	20	19	21	20	20	91	91.00
% Incorrect	0.00	4.00	5.00	0.00	0.00	9.00	

calls randomly from a single call distribution was rejected with a high degree of confidence ($\rho = 0.00\%$). Even more importantly, results of a jackknife test of *post-hoc* identification efficiency (Tab. 2) indicated that these discriminant functions are relatively stable and might be expected to return up to 90 percent accurate results for sets of unknowns drawn from statistically similar populations. As with the analysis of post-hoc training set discrimination, results of the jackknife test identifies the two *Myotis* species as being similar to one another in terms of call structure when assessed by the traditional spectrogram descriptor dataset.

In terms of gaining insight into the aspects of the traditional call variable sets responsible for the observed between-groups distinctions, because these CVA results are based on PCA scores, interpretation of the CVA space involves using the CVA eigenvector loading coefficients to interpret degree of alignment between the CVA axes and particular the PCA variables, and then using the PCA variables loadings to interpret degree of alignment between the CVA axes and particular sets of original variables. For variables expressed in differing units and that have little conceptual relation to one another, this is a daunting interpretive task; rarely attempted by even the most experienced CV data analysts. This task could simplified to some extent by using the original data as input directly into the CVA routine. However, doing this would forego the opportunity to achieve preliminary dimensionality reduction – which could be important for dataset that employ large numbers of descriptive variables. Indeed, for this dataset a direct CVA was not possible as the magnitudes of the variable values included in the traditional descriptor dataset differed by ten orders of magnitude, thus preventing the original matrix from being inverted.

Canonical Variates Analysis – Spectrogram Shape Coordinates

While ordination of the search echolocation calls within the the subspace formed by the first three CV axes of the eigensound form data (Fig. 10A) may appear similar to that of the traditional variables superficially, there are important differences. In Fig. 9 most between-groups separation occurred in the plane defined by CV 1 and CV 2. In the case of the geometric CVA analysis each of the first three canonical variates contribute to group separation. This is a much more balanced discriminant result than was found using the traditional data. In principle this
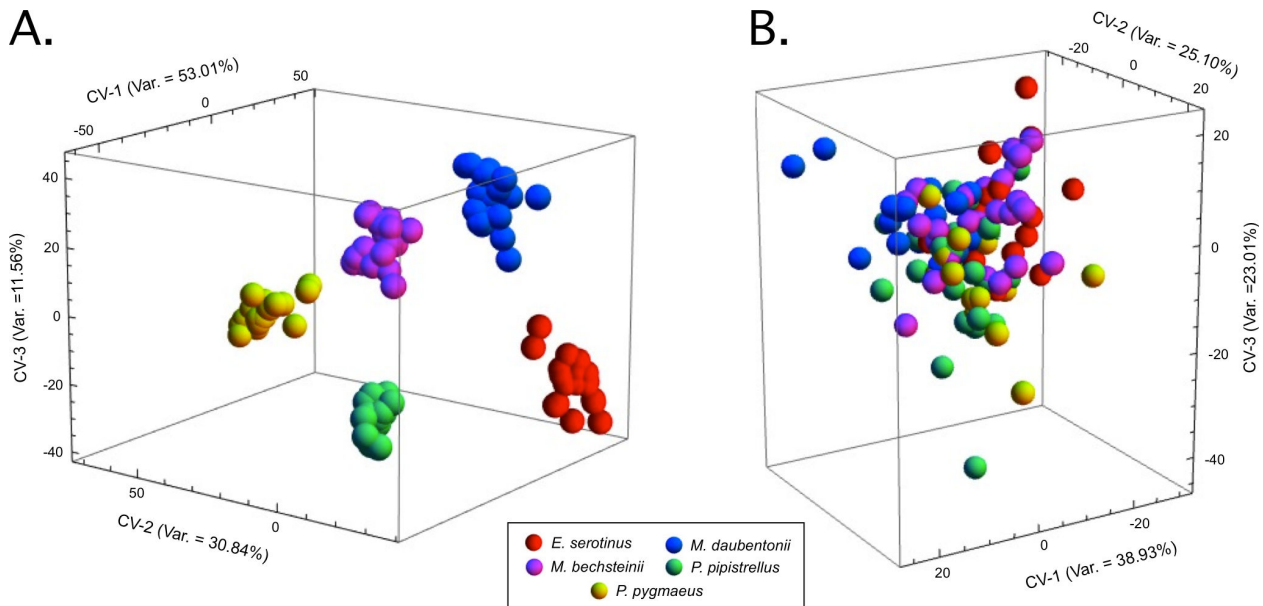
Figure 10 – Distribution of bat species call geometries in the subspace formed by the first three canonical variates of a 24 dimensional PC-based representation of spectrograph shape coordinates. A. Grouping variable set to reflect true species differences. B. Grouping variable set randomly in order to determine the degree with which the result presented in A could be consistent with the null hypothesis of no between-groups spectrogram shape differences. Note differences in the axis scales. See text for discussion.

should allow for a great degree of certainty in, and stability of, both group characterization and unknown call identification.

As before, *E. serotinus*, *P. pipistrellus*, and *P. pygmaeus* calls form tight, well-separated domains within the eigensound CV space (Fig. 10A). However using the eigensound variables the two *Myotis* species also separated cleanly into discrete and tightly clustered groups. This result is unprecedented in that *Myotis* species calls have proven to be resistant to separation based on traditional spectrogram descriptor variables even when analysed by themselves. To achieve such clear separations between the *Myotis* species' call structures when other species are present in the dataset suggests that a heretofore unexpected level of call distinctiveness exists between *Myotis* species. This interpretation is also consistent with the overall level of distinctiveness that appears to characterize the mean shape representations of *M. bechsteinii* and *M. daubentonii* in Fig. 6.

A log-likelihood ratio test for group centroid dispersion relative to within-groups variation rejects the the null hypothesis of no group-level structure to a high level of significance ($\Phi = 1051.00$, df = 232, $\rho = 0.00\%$), as does a 10000 pseudoreplicate Monte Carlo CVA designed to relax the distributional assumptions inherent in this parametric statistical test ($\Phi = 1045.42$, df = 112, critical value = 134.55, $\rho = 0.00\%$).

Despite the graphic result shown in Fig. 10A, some might question whether this grouping pattern can be used to refute the null hypothesis of no deterministic shape difference structure between groups owing to the relatively high dimensionality and relative modest number of individuals included in the dataset (see Bellman 1957; MacLeod 2007; Kovarovic et al. 2011). This issue can be resolved in two ways. First it is possible to repeat the analysis on the same set of data after the true group-level structure has been destroyed via randomized group membership assignments. The scatterplot obtained for this randomized-groups test is show in Fig. 10B. Note than randomising group membership resulted in complete destruction of group-specific spectrogram shape differences irrespective of the relatively high dimensionality of the dataset. These randomized data fail to pass a log-likelihood ratio test for the separation between group centroids ($\Phi = 106.10$, df = 112, $\rho = 63.96\%$) and exhibit a post-hoc efficiency of assigning members of the training set to their correct (randomized) groups as little better than would be expected due to chance alone (e.g., 50%, if there were just two groups).

The second test is to use a jackknife sampling strategy to examine the stability of the discriminant functions (Manly 1997, see Tab. 2). This test results in only nine individuals being misclassified post-hoc:

five *M. bechnsteinii* calls mistaken for *M. daubentonii* calls and four *M. daubentonii* calls were mistaken for *M. bechnsteinii*. While the jack-knifed cross-validation result is not perfect, it is well within the accuracy expectations of identifications based on other morphological data and far better than has been achieved by any similar analysis of bat echolocation call data previously. Further, these results suggest that, in addition to greater power of group characterization afforded by the eigensound approach to acoustic signal analysis, it may well be possible to conduct robust tests of systematic hypothesis with smaller sample sizes using geometric data than would be possible using a traditional set of spectrogram descriptors.

Perhaps best of all, use of geometric approaches to characterize spectrogram form allow for precise interpretations to be made of the geometric character of the discriminant space because it is an easy matter to project vectors the CVA space, the PCA space, and on into the space of the original variables (see MacLeod 2007, for a discussion of the projection equations). Figure 11 displays the results of using this method to illustrate the pattern of spectrogram shape variation along each of the first three geometric dataset CV axes.

Shape variation along CV axis 1 is strongly reminiscent of the patterns of shape variation captured by the first pooled groups eigensound axis (see Fig. 8). The polarity of these two axes is reversed, but eigenvector polarity is arbitrary, a by-product of the procedure used to estimate the eigenvectors. Other than this the pattern of shape change along these axes is almost identical, but with one important difference. Spectrogram surface shapes that project to positions high on CV axis 1 are characterized by long call durations and high duty cycling at low frequencies, but a sharply defined, broadband, multi-harmonic character. Given this characteristic spectrogram form it is readily understandable why the *E. serotinus* group projects to a position high on this axis. However, the opposite end of CV axis 1 in characterized by short duration, low duty cycling, frequency modulated calls accompanied by a single, low frequency, fundamental harmonic whose energy peak is realized quickly after call initiation. This is not the characteristic call form of *M. daubentonii*, which occupied the opposite end of the first eigensound axis, but rather of *M. bechsteinii*. Along this CV axis the broadband call typical of *M. daubentonii* occupies a position much closer to that of *E. serotinus* than to its congener *M. bechsteinii*.

Variation along CV axes 2 and 3 presents additional and even more subtle contrasts between spectrogram surface shapes, few of which could be understood in any detail without the graphical assistance provided by the eigensound spectrogram shape models. Along both
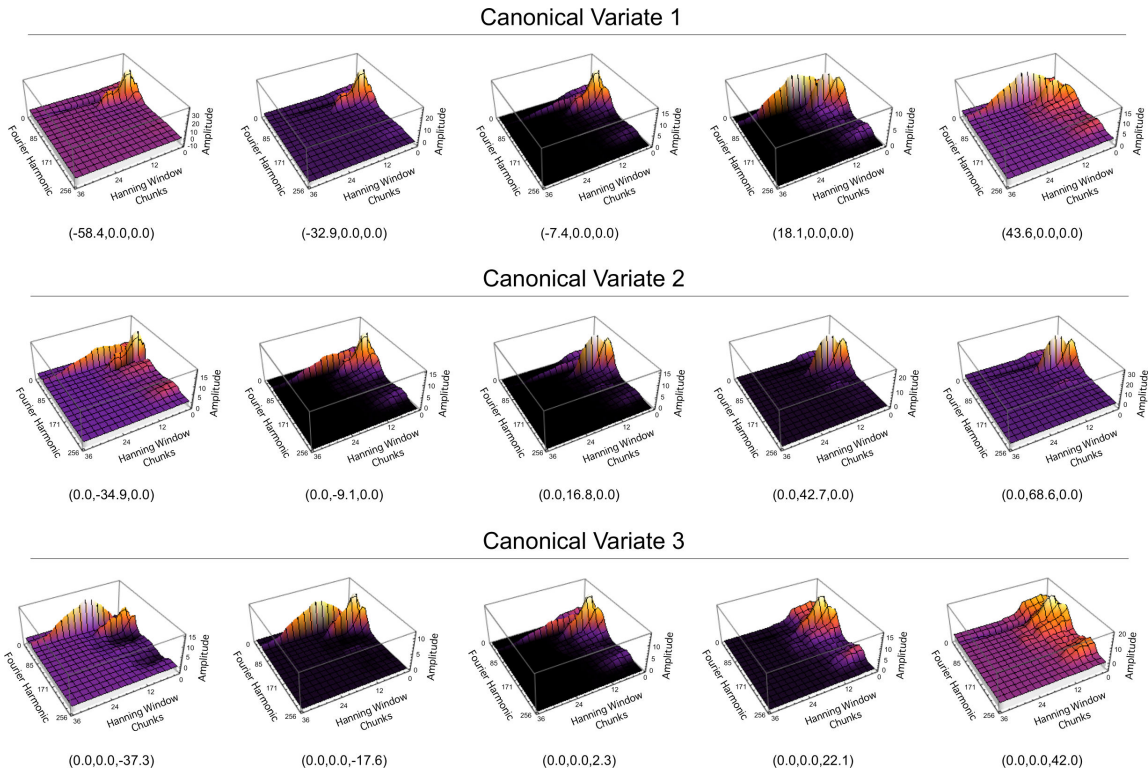
Canonical Variate 1

(-58.4,0.0,0.0)   (-32.9,0.0,0.0)   (-7.4,0.0,0.0)   (18.1,0.0,0.0)   (43.6,0.0,0.0)

Canonical Variate 2

(0.0,-34.9,0.0)   (0.0,-9.1,0.0)   (0.0,16.8,0.0)   (0.0,42.7,0.0)   (0.0,68.6,0.0)

Canonical Variate 3

(0.0,0.0,-37.3)   (0.0,0.0,-17.6)   (0.0,0.0,2.3)   (0.0,0.0,22.1)   (0.0,0.0,42.0)

Figure 11 – Hypothetical models of search call shape at a series of equally spaced coordinate positions (listed below each plot) along the first three CV axes. These models provide a visual aid for developing interpretations of the CVA space shown in Fig. 11. See text for discussion.

of these axes there is a contrast between long-duration, high duty-cycling, low frequency, biharmonic calls (low scores) with (CV axis 3) or without (CV axis 2) subsidiary higher frequency energy components and short calls with primary harmonics in the low-frequency band exhibit and energy peak in the very earliest call stage (CV axis 2) or throughout the early portion of the call (CV axis 1). Aside from these patterns there is a clear distinction between CV axis 2 and CV axis 3 in terms of the degree of frequency modulation they represent. This ranges from weak frequency modulation with strong attenuation (CV axis 2) to strong frequency modulation, but weak attenuation (CV axis 3). In the cases of both these axes the "middle ground" of the ordination spaces is characterised by relatively long duration, multi-harmonic calls with low frequency modulation overall. Given the patterns illustrated by these CV space models, not only can the ordination of group placement relative to each other be understood quickly and easily, reliable predictions can be made about call forms in (presently) unoccupied regions of the discriminant space.

Myotis Analyses

As a second demonstration of the flexibility and power of adopting a geometric approach to acoustic signal analysis we consider the case of European *Myotis*, a group of bats regarded as being very difficult to identify on the basis of call structure alone (Walters et al., 2012). These calls were collected at a sampling rate of 312500 Hz and a total (padded) duration of 0.01 seconds, parameters that yielded a sample of 3094 digitized values per call. All calls were amplitude standardized and transformed into a spectrogram using a 512 Hanning window with an offset of 128. For eigensound analysis these calls were down-sampled using a 25 cell grid, which reduced the effective dimensionality from 12800 spectrogram values to 625, or 5 percent of the total spectrogram information. Mean 3D spectrograms for each species are shown in Fig 12.

These down-sampled spectrogram data were processed according to the eigensound protocol (as outlined above) which focuses spectrogram shape information into a small number of composite geometric shape variables. For the *Myotis* dataset 29 eigensound variables/axes were needed to represent 95 percent of the observed 3D spectrogram

shape variation. Scores of each shape configuration across all 29 variables were submitted to a CVA to create a linear space that maximized between-groups separation relative to within-groups dispersion. A 3D plot of the subspace formed by the first three CV axes is shown in Fig. 13A as a way of illustrating the general character of between-groups separation that resulted from this analysis and that is resident with the spectrogram data for this sonically "difficult-to-characterize" multi-species group.

Within the low-dimensional subspace shown in Fig. 13A four species – *M. myotis*, *M. blythii*, *M. nattereri*, and *M. emarginatus* – all form tight, isolated clusters of call spectrogram geometries, well-separated
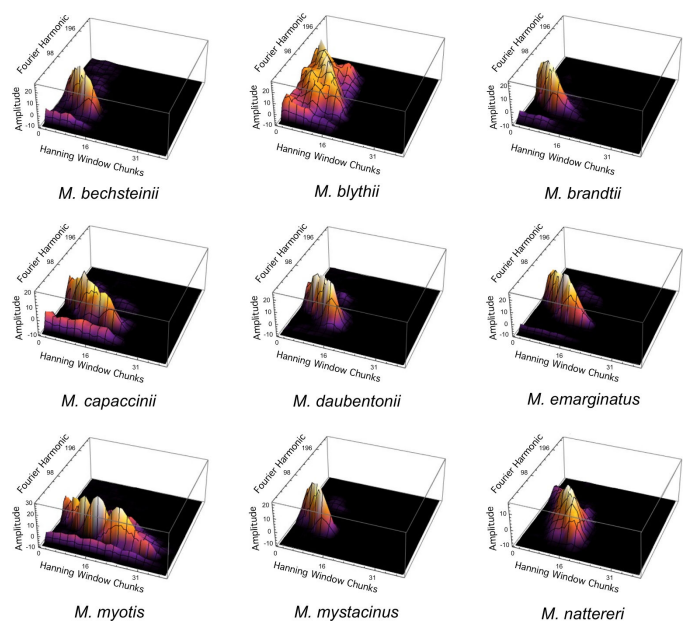

Figure 12 – Mean 3D spectrogram surface shapes that have been down-sampled to a 25 grid resolution for the nine *Myotis* species using in this investigation. These plots illustrate representative between-species call structure differences.

Table 3 – Confusion matrices for eigensound-based CVA results of call spectrogram form for *Myotis* species.

Raw cross-validation identifications of the training set specimens

Species	*M. bechsteinii*	*M. blythii*	*M. brandtii*	*M. capaccinii*	*M. daubentonii*	*M. emarginatus*	*M. myotis*	*M. mystacinus*	*M. nattereri*	**Total**	**% Correct**
M. bechsteinii	8				1			1		10	80.00
M. blythii		10								10	100.00
M. brandtii			9		1					10	90.00
M. capaccinii			1	9						10	90.00
M. daubentonii					10					10	100.00
M. emarginatus						10				10	100.00
M. myotis							10			10	100.00
M. mystacinus			1					9		10	90.00
M. nattereri									10	10	100.00
Total	8	10	11	9	12	10	10	10	10	90	94.44
% Incorrect	0.00	0.00	2.22	0.00	2.22	0.00	0.00	1.11	0.00		5.56

Jackknifed cross-validation identifications of the training set specimens

Species	*M. bechsteinii*	*M. blythii*	*M. brandtii*	*M. capaccinii*	*M. daubentonii*	*M. emarginatus*	*M. myotis*	*M. mystacinus*	*M. nattereri*	**Total**	**% Correct**
M. bechsteinii	7	1			1			1		10	70.00
M. blythii	2	7						1		10	70.00
M. brandtii	1		8		1				1	10	70.00
M. daubentonii			1		9					10	90.00
M. emarginatus				1		9				10	90.00
M. myotis							10			10	100.00
M. mystacinus		1	1		1			7		10	70.00
M. nattereri									10	10	100.00
Total	26	29	35	26	39	30	30	30	30	90	82.22
% Incorrect	3.33	2.22	3.33	1.11	4.44	1.11	0.00	3.33	0.00		17.78

Myotis myotis calls exhibit the greatest level of geometric distinction within the CV 1 to CV 3 subspace. This result is consistent with a visual inspection of the average spectrogram forms in Fig. 12. *Myotis myotis* obviously has the call of greatest mean duration relative to other species in the dataset. The very tight clustering of *M. myotis* call shape ordination evident in Fig. 13A indicates that this is a consistent feature of the species. Similarly, the mean calls of *M. blythii*, *M. nattereri* and *M. emarginatus* are all more similar to each other than any are to the mean *M. myotis* call, but nevertheless retain plainly distinctive features of their own in terms of their spectrogram surface geometries. For example *M. emarginatus* is characterized by a much narrower and more well-defined fundamental harmonic than is evident in the *M. blythii* call whereas the positioning and duration-frequency orientations of the *M. emarginatus* and *M. nattereri* fundamental harmonics all differ distinctively. Again, the tight clustering of these species groups in the discriminant spectrogram shape space suggests that these – and other – geometric feature(s) are consistent and distinctive call characteristics of these species. A log-likelihood ratio test of the *Myotis* discriminant space for significant group-centroid dispersion ($\Phi = 1051.00$, df = 232, $\rho = 0.00\%$) resulted in rejection of the null hypothesis of no group-level structure as does a 10000 pseudoreplicate Monte Carlo CVA designed to relax the distributional assumptions inherent in parametric statistical tests for group centroid separation relative to group dispersion ($\Phi = 1051.02$, df = 232, critical value = 236.60, $\rho = 0.00\%$).

As was the case with the more diverse sample (see above), the possibility exists that the relative high dimensionality of the dataset and low number of specimens may conspire to enable any combination of groups to appear significantly separated (see above). To address this issue a *Myotis* group-randomized dataset was created and subjected to CVA. A plot of the first three CV axes for these data is shown in Fig. 13B. As with the mixed-genus randomized group result, amalgamation of spectrograms from different species into the same group effectively destroys the group-level structure within the discriminant space. This lack of discriminatory power is also reflected in the results of the log-likelihood test for these randomized data ($\Phi = 197.20$, df = 232, $\rho = 95.28\%$) and in the confusion matrix that summarizes post-hoc discrimination performance (44 incorrect spectrogram assignments or 48.9% of the total).

On the basis of these results there is little question that the species-level call shape separations seen in Fig. 13A are consistent with the recognition of heretofore unanticipated, but nonetheless profound and statistically significant, levels of distinction between *Myotis* species' echolocation call structures. The efficiency of the *Myotis* discriminant functions in assigning these 90 calls to the correct groups *post-hoc* is impressive (Tab. 3; 94.4% correct identifications). Cross-validation of these results using the more rigorous jackknife strategy provides a
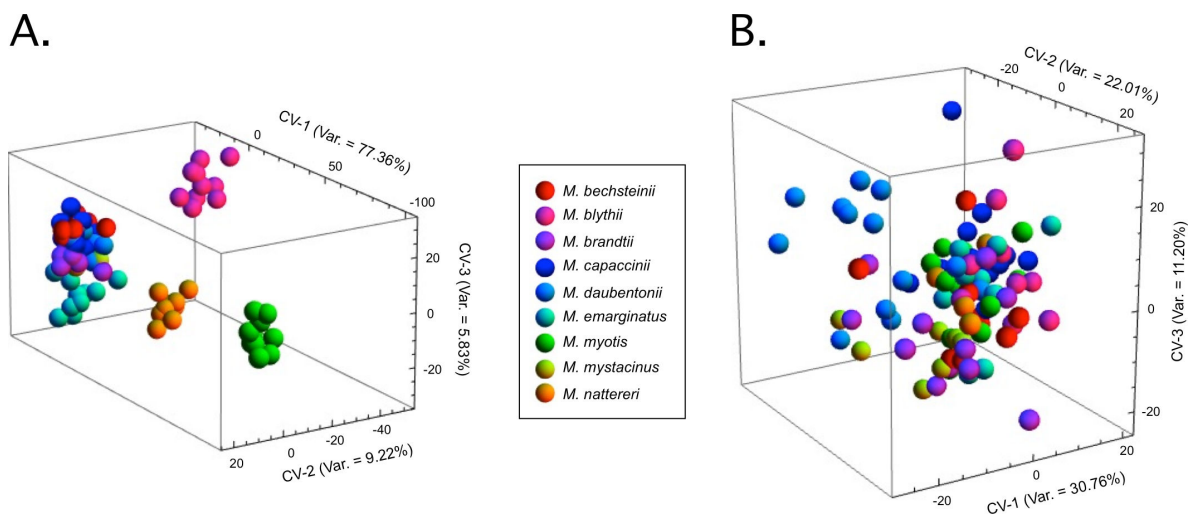
from each other and from a central cluster containing the remaining species. But even within the central cluster there is evidence of strong within-groups clustering and between-groups separation based on call structure. Again, there is no expectation that separations between all groups will be represented accurately within in this low-dimensional subspace. However, to see so many overt clusters in such a low-dimensional subspace is very encouraging in terms of the ability of a geometric approach to the analysis of call form to succeed in representing species-specific call distinctions in this widely acknowledged "difficult" species group.

Figure I3 – Distribution of *Myotis* species call geometries in the subspace formed by the first three canonical variates of a PCA-based summarization of their spectrograph shape coordinate data. A. Grouping variable set to reflect true species differences. B. Grouping variable set randomly in order to determine the degree with which the result presented in A could be consistent with the null hypothesis of no between-groups spectrogram shape differences. Note differences in the axis scales. See text for discussion.

more robust assessment of how the discriminant functions determined from this dataset might perform in a generalized context (Tab. 3, 82.2% correct identifications). But even given the circa ten percent decrease in identification performance under the more rigorous test, the result remains favourable especially given the small sample sizes involved in this study and when compared to previous attempts to characterize these species through echolocation call data alone (see below).

Discussion

Taken at face value these results underscore the potential of geometric morphometric approaches to play a significant role in a host of non-morphological (in a strict sense of that term) contexts. They become even more so when it is recalled that these results were generated by (1) quite small datasets and (2) quite a low level of 3D spatial resolution. Yet both mixed species and *Myotis* results have revealed a wealth of useful structure; structure that, up to now, had not been recognized, much less exploited successfully, to understand the systematics and biology of bat echolocation calls. Access to additional phenomenological levels in acoustic spectrogram data can be gained easily by increasing or decreasing the spatial resolution of the eigensound sampling grid. There is also scope for windowing of the sample grid itself in order to conduct analyses on mathematically isolated spatial components of spectrogram variation. Moreover, this generalized conceptualization, sampling, and geometric data-analysis strategy can be applied to any representation of any sort of acoustic data no matter how abstract or divorced from the anatomical roots of contemporary morphometric analysis.

In a previous investigation Lundy et al. (2011) claimed that their application of elliptical Fourier analysis (EFA) to aspects of the spectrogram of *M. daubentonii*, *M. mystacinus*, and *M. nattereri* calls represented the "first attempt to classify echolocation calls using morphometrics" (p. 103). As the generic term "morphometrics" applies to any and all attempts to quantify form and form change (see Blackith and Reyment 1971; Pimentel 1979), this claim is obviously false as it fails to acknowledge all prior attempts to quantify any aspect of bat sound – including the prior investigations cited by these authors in their own text. If this statement is taken to refer to GM, it is also questionable as, under some previous definitions of that term, EFA would be excluded because it does not operate in the Kendall shape space (see Bookstein 1990, 1991, p. 48).[1] However, the more important issue is to consider carefully which approach to the analysis of any given set of data is more appropriate for answering (in this case "the biological") questions raised successfully, adequately, and reliably.

The Lundy et al. (2011) investigation used EFA to characterize the form of the fundamental harmonic in the *Myotis* call spectrogram's frequency-duration plane. In *Myotis* species this harmonic forms only part of some species' characteristic call pattern (see Fig. 12). Indeed, it could be argued this harmonic sweep is so ill-defined as to be absent entirely in some *Myotis* species (e.g., *M. blythii*). Absent also is any criterion discussed by Lundy et al. (2011) by which the sweep's lower boundary – the boundary that controls the shape of the fundamental harmonic's outline – was determined objectively. As such, the outline of the fundamental harmonic in the spectrogram's frequency-duration plane seems a decidedly limited and problematic feature of the *Myotis* call to focus on for the purpose of sound characterization.

For those species in which the fundamental harmonic is present, its form is that of a long, narrow arc in the 3D spectrogram space. As is illustrated in Kuhl and Giardina (1982), EFA does not perform well when trying to characterize such structures. Since only 20 Fourier harmonics were used by Lundy et al. (2011) to describe the shape this structure it

is quite possible that distortions in the representation of these outlines were introduced by the EFA algorithm at both of the sharp ends of the fundamental harmonic's termini. Based on their Fig. 2-III the representations of these sweep patterns also seem to be of quite low resolution, with highly aliased boundaries and (so) distorted forms. Lundy et al. (2011) provided no information regarding the resolution of the semilandmark data used to quantify these outlines and/or what, if any, steps were taken to ensure both sides of the harmonic's trace were represented by an equivalent number of landmarks that occupy equivalent positions in the semilandmark sampling sequence across the sample (see MacLeod 1999 for a discussion of the problems that result for poor registration of outlines across a sample along with a simple strategy for correcting the problem). In addition, the Lundy et al. approach approach appears not to focus on locating the position of the fundamental harmonic within the context of the entire call structure.

Given these issues it is remarkable that the Lundy et al. (2011) EFA approach delivered even marginally adequate results. An overall identification accuracy of 79.6 percent was achieved using stepwise (but apparently a non-cross-validated) discriminant analysis of the EFA-based characterization of 2D sweep geometry alone. This accuracy estimate was later boosted to 96.3 percent via inclusion of the traditional spectrogram descriptive parameter "maximum frequency" in the data prior to stepwise discriminant analysis. Nevertheless, this approach to bat echolocation call analysis cannot be generalized even to all *Myotis* species – much less all bat species – insofar as multi-harmonic species cannot be represent by a single harmonic sweep outline. The eigensound approach to acoustic signal shape analysis circumvents all these issues, simply, elegantly, and effectively as well as delivering superior results.

In eigensound analysis, standardization of the spatial representation of the entire call sound structure is achieved by adopting the convention that each sound file starts at call initiation, each ends at the end of the normal signal duration (so no part of the sound is stretched or compressed artificially), and by ensuring that sound files are of equivalent duration by adding silence to the ends of the shorter-duration calls. The former is comparable in the anatomical morphometric realm to beginning outline digitization at a single landmark point that corresponds to all other call initiation landmarks across the sample. The latter is effectively analogous to ensuring all calls are set to the same "size" in the sense of being represented by the same number of Fourier harmonic amplitude variables. In this sense acoustic homology is maintained across the entire dataset in terms of the physical energy-duration "form" of the call. Re-expression of the sound's information content using a set of Fourier coefficients spatially organized into a Hanning window corresponds to the re-expression of a boundary outline curve using any radial or elliptical Fourier spectra, or indeed the the re-expression of a landmark-based shape configuration by means of principle/partial warps. Use of a grid-based representation of the sound structure also ensures equivalent spatial dimensionality across all sounds included in the sample and represents the conceptually equivalent of a Procrustes alignment (without the need to actually perform the Procrustes calculations). Finally, subsampling this spectrograph grid to reduce the effective dimensionality of the data, along with use of the baseline adjustment convention, represents the sonic equivalent of standard digital image processing procedures designed to boost the effective signal-to-noise ratios of the spectrograms.

To appreciate the similarities and the differences between this method of spectrogram processing the data processing steps considered routine in GM it is important to note that each of the steps outline above is performed on individual sound files without reference to any information contributed by the sample itself. In other words, no part of these operations is optimized via reference to any other sound or sound spectrogram in the sample. While it is tempting to use the term "homology" (in its mathematical sense of spatial correspondence) to describe the equivalence between grid cells in the down-sampled Hanning grid, in order to avoid confusion the reader may want to regard these positional equivalents simply as "windowing correspondences". Similar sampling strategies are also key parts of eigensurface

---

[1] Adams et al. (2004) claimed that "Outline methods were the first geometric morphometric methods to be used" (p. 6), but defined GM very simplistically, as little more than a set of multivariate procedures that operate on "Data that captured the geometry of the morphological structure" (also p. 6). By this rather general (and generous) definition, virtually any data collected from an organismal body – including linear distances between landmarks (see Strauss and Bookstein 1982), and any numerical data-analysis procedure could be regarded as being consistent with the principles of GM (see also arguments presented in the Introduction).

analysis (MacLeod, 2008; Sievwright and MacLeod, 2012) and certain approaches to machine learning (MacLeod et al., 2007a,b; MacLeod, 2012). Even after using such severe down-sampling schemes as those employed in this investigation, all of the traditional spectrogram descriptor variable concepts are represented in one form or another in the gridded eigensound dataset and so are part of the the overall eigensound analysis. In addition to this, a wealth of other geometric information not captured by either traditional sets of spectrogram scalar descriptors or the Lundy et al. (2011) EFA approach are also present in the eigensound data.

The results achieved through employment of the eigensound sampling and data characterization strategy speak for themselves regarding this technique's effectiveness. Any acoustic signal pattern, no matter how short, how long, or how complex – indeed any type of data that can be expressed as a matrix of objects and variables – can be treated in exactly the same manner and will likely deliver results of comparable sensitivity. In particular, the shape modeling capabilities of eigensound analysis represent a significant advance in the ability of mathematically complex ordination spaces to be assessed, interpreted, and used to facilitate communication with others about the nature of these spaces in a simple, informative, and intuitive visual manner (see also MacLeod 2002, 2008).

Once echolocation calls have been quantified using the eigensound approach it becomes possible to address a wide variety of questions pertinent to improving our understanding of bat systematics, ecology, functional morphology, and phylogenetics. For example, it has long been accepted that the form of bat echolocation calls has been determined by the functional needs of hunting particular prey in particular environments (e.g., Schnitzler and Kalko 2001; Jones and Teeling 2006). However, this assumption has been challenged recently by Collen (2012). Part of the problem in studying the phylogenetics of bat echolocation is the comparative lack of sufficiently detailed descriptive lexicon that can be used to identify call characters and character states (see Fig. 4 for an illustration). Treatment of call spectrograms as complex 3D morphological structures will facilitate their description using morphological terms for which there is a much richer vocabulary than is available in the traditional qualitative or semi-quantitative sound-description domains.

In performing such an analysis there is an implicit assumption that call structures of similar form are produced by biologically homologous physical structures, behaviours, physiological responses to external stimuli, functional constraints, etc. However, as has been demonstrated repeatedly in the contexts of comparative method and phylogenetic studies, the extent to which this assumption is justified cannot be decided *a priori* based on the nature of the putative character or its mode of description. Rather this is an empirical question that can be answered only by carrying out the analyses required to demonstrate (or not) the existence of phylogenetically structured patterns of variation in characters or variables derived, in this case, from the audio signal. But irrespective of the results that may be obtained from a test of this hypotheses, the point we are making here is that the eigensound approach to the representation, summarization, analysis, and comparison of the echolocation call's physical signal structure facilitates these types of analyses in a manner that makes it possible to describe sounds either as sets of continuous variables (e.g., Hanning window correspondences) or, depending on the structure of variation within a set of sampled spectrograms, a series of quantified geometric characters and character states rather than a series of imprecise categorical assessments (e.g., high duty cycling-low duty cycling, high frequency-low frequency, attenuated-non attenuated) based on the qualitative assessments of spectrogram patterns or via reference to crude descriptive indices (e.g., highest frequency, lowest frequency, bandwidth).

Along these same lines, quantification of bat call form will provide data analysts with the ability to exert direct control over the degree to which comparisons based on acoustic data are influenced by the phylogenetic component of cross-species call comparisons. The mappings of call form categories offered by Jones and Teeling (2006) and by Collen (2012) show that, to varying degrees, all bat calls should be expected to have component of phylogenetic covariance embedded within their structure. Felsenstein (1985, 1988, 2002); Harvey and Pagel (1991); Harvey et al. (1996); Martins and Hansen (1997); MacLeod (2001); Rohlf (2001, 2002, 2006) and a host of others have all made the case that the analysis of morphological, behavioral, ecological, and geographical data must take phylogenetic covariance into consideration when designing quantitative tests of biological hypotheses or run the risk of introducing substantial error in the results produced. Lack of a reliable and sufficiently detail approach to the quantification of acoustic data has, to date, kept bioacoustic signal analysis from taking advantage of improved statistical testing and data-analysis strategies that are robust to the effects of phylogenetic structure (e.g., Revell 2009). The eigensound approach to acoustic signal analysis provides a means by which the advantages of comparative method procedures can be introduced into the field of bioacoustic analysis.

Last but by no means least, the quantitative representation of acoustic structure is a prerequisite for the construction of reliable automated species identification systems for use in bat biodiversity and bat conservation studies. The bat systematics community is well ahead of other areas of biology in recognizing the important role such systems will play in twenty-first century biological research. The assembly of such systems presumes the existence a generalized approach to the identification and assessment of within-groups similarities, and between-groups differences among species. Any approach that employs one set of variables to identify one group of species, but another set to identify others, cannot be turned into a fully automated system easily (see Walters et al. 2012). However, the to the extent that sonogram data can be used to represent the information content of bat echolocation calls, the eigensound approach is fully generalizable and can be used as a complete and sufficient system for representing, partitioning, and identifying bat species on the basis of the sonic structure of their calls. Indeed, the computational overhead required by an eigensound-based system is relatively modest; well within the range of most high-end smartphone processors (e.g., Apple iPhone). Moreover, any phone with wifi capability can be used to upload a call record and control the server software that would be required to perform the necessary calculations with results being displayed as a web page.

While the eigensound results reported here by no means solve the "bat identification from echolocation call problem" in general or the "*Myotis* problem" in particular, they are the best results that have been obtained to date and the first to reveal that such clear distinctions between different *Myotis* species calls exist. The fact that excellent between-species separations based on call structure were obtained for both *Myotis*-only datasets and mixed-species datasets is unprecedented. Indeed, the clear improvement in *Myotis* species identifications produced using the eigensound approach suggests that the *Myotis* problem may have more to do with the descriptive variables that have been used traditionally to characterize bat echolocation calls than with the fundamental structure of the calls themselves. Additional research in the area of call characterization is now needed, both in terms of testing the eigensound approach with larger species training sets, and testing alternative algorithms that are consistent with the geometric philosophy that stands behind eigensound's basic approach to acoustic signal characterization and analysis; especially those designed to cope with non-linear patterns of variation that may be present with bat echolocation call data (see MacLeod et al. 2007a,b; MacLeod 2007, 2012 and above).

Summary and conclusions

In this report we have taken up the issue of acoustic signal analysis and asked what (if anything) geometric morphometrics can contribute to the study of sounds. In particular we have employed a "eigensound analysis" – a Procrustes PCA applied to a spectrogram-based 3D characterization of sound structure – to analyze similarities and differences within two datasets of bat search calls, a mixed set of five species and four genera including both easy and challenging call types and a more uniform set of nine species from a single genus, *Myotis*, which is widely acknowledged to be difficult to identify to the species level based on traditional spectrogram descriptor variables. In both cases

the eigensound approach achieved excellent results, detecting complete between-groups separation for the training set sample in the first dataset and in the second to an overall accuracy of 94 percent. These results demonstrate the reality of species-specific distinctions between gross call structures. However, for the purpose of evaluating what level of performance might be realized as a result of the use of these discriminant functions to identify unknown bat calls the cross-validated and jackknifed results are more pertinent. As is typical in such analyses, these more robust assessments of discriminant function performances achieve c. 10 percent lower accuracy estimates when compared to results obtained from analyses of the original training set. We hasten to point out that we are not advocating the discriminant functions obtained during the course in our investigation be used for identifying bat species from their echolocation calls. Our results are indicative only of the type of results that might be realized using a larger bat call training set. Irrespective of this caveat though, so far as we are aware these are the best results that have been achieved to date for bat echolocation calls using any approach to spectrogram form characterization and/or analysis. Jackknifed cross-validation analyses of these data also indicate that the discriminant function systems specified as a result of this small example analysis are surprisingly robust and would be useful in automating bat species identifications based on echolocation call data alone.

Furthermore, the results reported above also address several other important issues. First, that species specific information is encoded in bat echolocation call structures in sufficient quantities to facilitate reliable species identification; even in the case of those species groups (e.g., *Myotis*) that have resisted such characterization in the past. Second, the strategy of successive focusing of the information content of a set of echolocation spectrograms through use of (a) 3D surface sampling grids and (b) PCA (or SVD) transformation can result in massive reductions in the dimensionality of the spectrogram analysis problem with little or no apparent loss in the ability of such reduced datasets to identify even difficult-to-identify species' echolocation calls successfully. Third, use of the shape modeling techniques (that have been pioneered by morphometricians) in the analysis and interpretation of spectrograph data opens the door to a new level of understanding of the complex geometric spaces within which a a wide variety of data reside. Such visualizations are simply not possible when using traditional sets of (largely scalar) spectrogram descriptor variables. More comprehensive, systematic, and sensitive quantification of spectrogram data may eventually allow the study of natural sounds (bioacoustics) to become a subject for evolutionary biologists to study by taking advantage of numerous procedures whose effectiveness – even when analysing complex data in which the concept of biological homology applies only in the loosest of terms (e.g., behavioural data, social data, cognition data) has already been demonstrated. These include the following:

i) comparative method studies that are necessary to improve the statistical testing of bioacoustic data by explicitly identifying phylogenetic covariation and incorporating these factors into the design of statistical procedures;

ii) methods that seek to identify the structure of covariance patterns between bioacoustic data and morphological data, genetic data, geographic data, ecological data, and indeed other acoustical data (e.g., to analyse patterns of correlation between the sounds made by animals and aspects of their phylogeny, ecology, behaviour, linguistic style);

iii) as a potentially new source of information for testing phylogenetic hypotheses and understanding the history of life on Earth.

At the most general level, the results achieved by this investigation suggest that geometric morphometrics can transcend its roots in biological morphology and address important questions in fields that, on first inspection, are not currently regarded as being morphological in nature. These include research programmes in other areas of the biological sciences, in the physical sciences, and possibly even in the social sciences and humanities (e.g., MacLeod 2009b).

Geometry is a fundamental aspect of the world in which we live. Owing to our own evolutionary history we have an affinity for conceptualizing the patterns we observe in geometric terms. The tools of shape theory and geometric analysis, forged as a result of the development of geometric morphometrics, have provided the scientific community with a set of data-analysis instruments of unlimited potential in terms of its range of conceivable applications. In order to push the morphometrics revolution forward into the twenty-first century morphometricians need to understand both the generalized nature of the tools they possess and the geometric dimensions of the interesting questions that exist in research fields far removed from morphometrics' traditional home in systematic biology. By expanding the scope of scientific problems that can be addressed by geometric morphometric methods the morphometrics community can not only make important contributions in areas far removed from its "local neighbourhood" of anatomy-based biological sciences, it can help reconceptualize problems across the physical, chemical, and humanistic sciences, demonstrate the ubiquity of morphological patterns throughout the nature, and bring some of the most sophisticated analytic approaches in the whole of applied mathematics to be bear on their resolution. They can, in a word, continue the ongoing morphometrics revolution, a continuation that will reap benefits for morphometics and morphometricians, as well as for those working in the fields to which these methods may be applied. ☞

References

Adams D., Rohlf F.J., Slice D.E., 2004. Geometric morphometrics: ten years of progress following the "revolution": Italian Journal of Zoology 71: 5–16.

Aston J.D., Buck D., Coleman J., Cotter C.J., Jones N.S., Macaulay V., MacLeod N., Moriary J.M., Nevins J., 2012. Phylogenetic inference for function-valued traits: speech sound evolution: Trends in Ecology and Evolution 27(3): 160–166.

Blackith R.E., Reyment R.A., 1971. Multivariate morphometrics. Academic Press, London.

Bellman R.E., 1957. Dynamic programming. Princeton University Press, Princeton.

Bolton S., Edgecombe G.D., MacLeod N., 2008. Variability in female gonopods of scutigeromorph centipedes (Chilopoda): a geometric morphometric approach. Pecking 6: 97.

Bookstein F.L., 1990. Analytic Methods: Introduction and Overview, In: Rohlf F.J., Bookstein F.L. (Eds.) Proceedings of the Michigan Morphometrics Workshop. The University of Michigan Museum of Zoology, Special Publication 2, Ann Arbor, MI. 61–74.

Bookstein F.L., 1991. Morphometric tools for landmark data: geometry and biology. Cambridge University Press, Cambridge.

Bookstein F.L., 1993. A brief history of the morphometric synthesis. In: Marcus L.F., Bello E., García-Valdecasas A. (Eds.) Contributions to Morphometrics. Museo Nacional de Ciencias Naturales 8, Madrid. 18–40.

Bookstein F.L., 1997. Landmark methods for forms without landmarks: Localizing group differences in outline shape. Medical Image Analysis 1: 225–243.

Campbell N.A., Atchley W.R., 1981. The geometry of canonical variate analysis. Systematic Zoology 30: 268–280.

Collen A., 2012. Evolution of bat echolocation. PhD Dissertation. University College London, London.

Cramer C.J., 2004. Essentials of computational chemistry: theories and models, 2nd Edition. Wiley, New York.

Dryden I.L., Mardia K.V., 1998. Statistical shape analysis. Wiley, New York.

Felsenstein J., 1985. Phylogenies and the comparative method. American Naturalist 125: 1–15.

Felsenstein J., 1988. Phylogenies and quantitative characters. Annual Review of Ecology and Systematics 19: 445–471.

Felsenstein J., 2002. Quantitative characters, phylogenies, and morphometrics. In: MacLeod N., Forey P.L. (Eds.) Morphology, shape and phylogeny. Taylor & Francis, London. 27–44.

Fenton M.B., Audet D., Obrist M.K., Rydell J., 1995. Signal strength, timing and self deafening: the evolution of echolocation in bats. Paleobiology 21: 229–242.

Ferson S., Rohlf F.J., Koehn R.K., 1985. Measuring shape variation of two-dimensional outlines. Systematic Zoology 34(1): 59–68.

Franklin S.E., Maudie A.J., Lavigne M.B., 2001. Using spatial cooccurrence texture to increase forest structure and species composition classification accuracy. Photogrammetric Engineering and Remote Sensing 67(7): 849–855.

Friston K., Phillips J., Chawla D., Büchel C., 2000. Nonlinear PCA: characterizing interactions between modes of brain activity. Philosophical Transactions of the Royal Society, Series B (Biological Sciences) 355: 135–146.

Greenacre M.J., 1984. Theory and applications of correspondence analysis. Academic Press, London.

Gunz P., Mitteroecker P., Bookstein F.L., 2005. Semilandmarks in three dimensions. In: Slice D.E. (Ed.) Modern Morphometrics in Physical Anthropology. Kluwer Academic/Plenum Publishers, New York. 73–98.

Hammer Ø., Harper D., 2006. Paleontological data analysis. Blackwell Publishing, Oxford, UK.

Harris F.J., 1978. On the use of windows for harmonic analysis with the discrete Fourier transform. Proceedings of the IEEE 66(1): 51–83.

Harvey P.H., Leigh Brown A.J., Smith J. M., Nee S., 1996. New uses for new phylogenies. Oxford University Press, Oxford.

Harvey P.H., Pagel M.D., 1991. The comparative method in evolutionary biology. Oxford University Press, Oxford.

Jones G., 1999. Scaling of echolocation call parameters in bats. Journal of Experimental Biology 202: 3359–3367.

Jones K.E., Russ J.A., Bashta A.-T., Bilhari Z., Catto C., Csösz I., Gorbachev A., Györfi P., Hughes A., Ivashkiv I., Koryagina N., Kurali A., Langton S., Maltby A., Margiean G., Pandourski I., Parsons S., Prokofev I., Szodoray-Paradi A., Szodoray-Paradi F., Tilova

E., Walters C., Weatherill A., Zavarzin O. 2013. Indicator Bats Program: a system for the global acoustic monitoring of bats, In: Collen B.P., Pettorelli N., Durant S.M., Krueger L., Baillie J. (Eds.) Biodiversity monitoring and conservation: bridging the gaps between global commitment and local action. Wiley-Blackwell, London. 213–247.

Jones G., Teeling E.C., 2006. The evolution of echolocation in bats. Trends in Ecology & Evolution 21(3): 149–156.

Kalko E.K.V., Schnitzler H.U., 1993. Plasticity in echolocation signals of European pipistrelle bats in search flight: implications for habitat use and prey detection. Behavioral Ecology and Sociobiology 33(6): 415–428.

Kayitakire F., Hamel C., Defourny P., 2006. Retrieving forest structure variables based on image texture analysis and IKONOS-2 imagery. Remote Sensing of Environment 2006: 390–401.

Kendall D.G., 1984. Shape manifolds, procrustean metrics and complex projective spaces. Bulletin of the London Mathematical Society 16: 81–121.

Klingenberg C.P., 2008. Novelty and "homology-free" morphometrics: what's in a name. Evolutionary Biology 35: 186–190.

Kovarovic K., Aiello L.C., Cardini A., Lockwood C.A., 2011. Discriminant function analyses in archaeology: are classification rates too good to be true? Journal of Archaeological Science 38: 3006–3018.

Kramer M.A., 1991. Nonlinear principal component analysis using autoassociative neural networks. AIChE Journal 37(2): 233–243.

Kuhl R.K.J., Giardina C.R., 1982. Elliptic Fourier features of a closed contour. Computer Graphics and Image Processing 18: 236–258.

Lohmann G.P., 1983. Eigenshape analysis of microfossils: A general morphometric method for describing changes in shape. Mathematical Geology 15: 659–672.

Lundy M., Teeling E., Boston E., Scott D., Buckley D., Prodohu P., Marnel F., Montgomery I., 2011. The shape of sound: elliptic Fourier descriptors (EFD) discriminate the echolocation calls of *Myotis* bats (*M. daubentoni*, *M. nattereri* and *M. mystacinus*). Bioacoustics 20: 101–116.

MacLeod N., 1999. Generalizing and extending the eigenshape method of shape visualization and analysis. Paleobiology 25(1): 107–138.

MacLeod N., 2001. The role of phylogeny in quantitative paleobiological analysis. Paleobiology 27: 226–241.

MacLeod N., 2002. Phylogenetic signals in morphometric data. In: MacLeod N., Forey P.L. (Eds.) Morphology, shape and phylogeny. Taylor & Francis, London. 100–138.

MacLeod N., 2006. Rs and Qs II: correspondence analysis. Palaeontological Association Newsletter 62: 60–74.

MacLeod N., 2007. Groups II. Palaeontological Association Newsletter 65: 36–49.

MacLeod N., 2008. Understanding morphology in systematic contexts: 3D specimen ordination and 3D specimen recognition. In: Wheeler Q. (Ed.) The New Taxonomy. CRC Press, Taylor & Francis Group, London. 143–210.

MacLeod N., 2009a. Form & shape models. Palaeontological Association Newsletter 72: 14–27.

MacLeod N., 2009. Images, totems, types and memes: perspectives on an iconological mimetics. Culture, Theory and Critique 50(2–3): 185–208.

MacLeod N., 2012. The center cannot hold II: elliptic Fourier analysis. Palaeontological Association Newsletter 79: 29–42.

MacLeod N. (in press). A comparison of alternative form-characterization approaches to the automated identification of biological species. In: Hamilton A., Peirson E. (Eds.) Patterns in Nature. University of California Press, Berkeley, California.

MacLeod N., O'Neill M.A., Walsh S.A., 2007a. A comparison between morphometric and artificial neural net approaches to the automated species-recognition problem in systematics. In: Curry G., Humphries C. (Eds.) Biodiversity databases: techniques, politics, and applications. CRC Press, Taylor & Francis Group, Boca Raton, Florida. 37–62.

MacLeod N., O'Neill M.,Walsh S.A., 2007b. Automated tools for the identification of taxa from morphological data: face recognition in wasps. In: MacLeod N. (Ed.) Automated taxon recognition in systematics: theory, approaches and applications. CRC Press, Taylor & Francis Group, Boca Raton, Florida. 153–188.

Manly B.F.J., 1994. Multivariate statistical methods: a primer. Chapman & Hall, Bury, St. Edmonds, Suffolk.

Manly B.F.J., 1997. Randomization, bootstrap and Monte Carlo methods in biology. Chapman & Hall, London.

Mardia K.V., Dryden I., 1998. The statistical analysis of shape data. Biometrika 76: 271–282.

Martins E.P., Hansen T.F., 1997. Phylogenies and the comparative method: a general approach to incorporating phylogenetic information into the analysis of interspecific data. American Naturalist 149: 646–667.

Oxnard C., O'Higgins P., 2008. Biology clearly needs morphometrics. Does morphometrics need biology? Biological Theory 4(1): 84–97.

Parsons S., Jones G., 2000. Acoustic identification of twelve species of echolocating bat by discriminant function analysis and artificial neural networks. The Journal of Experimental Biology 203: 2641–2656.

Pielou E.C., 1984. The interpretation of ecological data. John Wiley & Sons, New York.

Pimentel R.A., 1979. Morphometrics: the multivariate analysis of biological data. Kendall/Hunt, Dubuque, IA.

Podani J., Miklós I., 2002. Resemblance coefficients and the Horseshoe Effect in principal coordinates analysis. Ecology 83: 3331–3343.

Polly P.D., 2008. Adaptive zones and the pinniped ankle: a 3D quantitative analysis of carnivoran tarsal evolution. In: Sargis E., Dagosto M. (Eds.) Mammalian Evolutionary Morphology: A Tribute to Frederick S. Szalay. Springer, Dordrecht, The Netherlands. 165–194.

Polly P.D., MacLeod N., 2008. Locomotion in fossil Carnivora: an application of the eigensurface method for morphometric analysis of 3D surfaces. Palaeontologia Electronica 11(2): 13.

Redgewell R.D., Szewczak J. M., Jones G., Parsons S., 2009. Classification of echolocation calls from 14 species of bat by support vector machines and ensembles of neural networks. Algorithms 2: 907–924.

Revell L.J., 2009. Size-correction and principal components for interspecific comparative studies. Evolution 63(12): 3258–3268.

Reyment R.A., 1991. Multidimensional paleobiology. Pergamon Press, Oxford.

Reyment R.A., Jöreskog K.G., 1993. Applied factor analysis in the natural sciences. Cambridge University Press, Cambridge.

Rohlf F.J., 2001. Comparative methods for the analysis of continuous variables: geometric interpretations. Evolution 55(11): 2143–2160.

Rohlf F.J., 2002. Geometric morphometrics and phylogeny. In: MacLeod N., Forey P.L. (Eds.) Morphology, shape and phylogeny. Taylor & Francis, London. P175–193.

Rohlf F.J., 2006. A comment on phylogenetic correction. Evolution 60(7): 1509–1515.

Rohlf F.J., Slice D., 1990. Extensions of the Procrustes method for optimal superposition of landmarks. Systematic Zoology 39: 40–59.

Rohlf F.J., 1993. Relative warp analysis and an example of its application to mosquito wings. In: Marcus L.F., Bello E., García-Valdecasas A. (Eds.) Contributions to Morphometrics. Museo Nacional de Ciencias Naturales 8, Madrid. 131–160.

Roiu R., Seyler F., 1997. Texture analysis of tropical rainforest infrared satellite images: application to structural geology and soil studies. Photogrammetric Engineering and Remote Sensing 63(5): 515–521.

Russ J., 2012. British Bat Calls: A Guide to Species Identification. Pelagic Publishing, Exeter, UK.

Schnitzler H.U., Kalko E.K.V., 2001. Echolocation in insect-eating bats. Bioscience 51: 557–569.

Schölkopf B., Smola A., Müller K.-R., 1998. Nonlinear component analysis as a kernel eigenvalue problem. Neural Computation 10(5): 1299–1319.

Scholz M., Fraunholz M., Selbig J., 2007. Nonlinear principal component analysis: neural network models and applications. In: Alexander N., Gorban A.N., Kégl B., Wunsch D. C., Zinovyev A. (Eds.) Lecture Notes in Computational Science and Engineering. Volume 58: 44–67.

Sievwright H., MacLeod N., 2012. Eigensurface analysis, ecology, and modeling of morphological adaptation in the falconiform humerus (Falconiformes: Aves). Zoological Journal of the Linnean Society 165: 390–415.

Strauss R.E., Bookstein F.L., 1982. The truss: body form reconstruction in morphometrics. Systematic Zoology 31: 113–135.

Supa M., Cotzin M., Dallenbach K.M., 1944. "Facial vision" – the perception of obstacles by the blind. The American Journal of Psychology 57(2): 133–183.

Teeling E.C., 2009. Hear, hear: the convergent evolution of echolocation in bats? Trends in Ecology & Evolution 24(7): 351–354.

Thaler L., Arnott S.R., Goodale M. A., 2011. Neural correlates of natural human echolocation in early and late blind echolocation experts. PLOS One 6(5): 1–16.

Vaughan N., Jones G., Harris S., 1997. Identification of british bat species by multivariate analysis of echolocation call parameters. Bioacoustics 7(3): 189–207.

Walters C.L., Freeman R., Collen A., Dietz C., Fenton M.B., Jones G., Obrist M.K., Puechmaille S.J., Sattler T., Siemers B.M., Parsons S., Jones K.E., 2012. A continental-scale tool for acoustic identification of European bats. Journal of Applied Ecology 49(5): 1064–1074.

Young D., 2001. Computational chemistry: a practical guide for applying techniques to real world problems. Wiley, New York.

Associate Editor: A. Cardini